Title
The role of host inflammation and the commensal microbiota in the pathogenesis of medication-related osteonecrosis of the jaw

Author
Williams, Drake

Publication Date
2019

Peer reviewed|Thesis/dissertation

UNIVERSITY OF CALIFORNIA

Los Angeles

The role of host inflammation and the commensal microbiota in the pathogenesis of medication-related osteonecrosis of the jaw

A dissertation submitted in partial satisfaction of the

requirements for the degree Doctor of Philosophy

in Oral Biology

by

Drake Winslow Williams

2019

ABSTRACT OF THE DISSERTATION

The role of host inflammation and the commensal microbiota in the pathogenesis of medication-related osteonecrosis of the jaw

by

Drake Winslow Williams

Doctor of Philosophy in Oral Biology

University of California, Los Angeles, 2019

Professor Reuben H. Kim, Chair

Bisphosphonates (BPs) and denosumab (Dmab) are anti-resorptive drugs that are clinically used to treat bone disorders like osteoporosis and bone metastases. A detrimental side effect of these drugs that uniquely occurs in the oral cavity is BP- and Dmab-related osteonecrosis of the jaw (collectively called medication-related osteonecrosis of the jaw, or MRONJ), clinically defined as exposed necrotic bone with unclosed overlaying oral mucosa for at least 8 weeks. Although the first report of ONJ by BPs appeared in 2003, the exact pathophysiology of MRONJ is still largely unknown. Our laboratory has been working to examine and elucidate the pathophysiology of MRONJ. Previously, we established mouse models for MRONJ utilizing bisphosphonate and αRANKL antibody and identified that woven bone formation and inhibition of bone resorption are hallmarks of murine MRONJ lesions. We also utilized semi-unbiased gene profiling to identify and validate the importance of IL36 signaling in MRONJ pathogenesis.

MRONJ often occurs following a dental intervention such as a tooth extraction which is typically performed to eliminate localized periodontal or periapical inflammation. Periodontal

disease is caused by polymicrobial infection and subsequent host immune response; thus, we hypothesize that local inflammation driven by host responses plays a critical role in MRONJ development. In this study, we found that 1) Long-term (10 weeks) ligature-induced periodontitis (L-LIP) exacerbates bone loss and local expression of *Il17a*; 2) Host response, not microbial community composition, drives bone loss in L-LIP; and 3) L-LIP combined with BP and extraction leads to significantly more necrotic bone formation than short-term (3 weeks) ligature-induced periodontitis. Additionally, we utilized a microbiota-depletion model to identify the role of the commensal microbiota in inflammation-induced osteonecrosis development and found that 1) MRONJ lesions have an increased number of infiltrating bacteria compared to vehicle controls; 2) The commensal microbiota partially protects against the development of osteonecrosis following extraction of periodontally diseased teeth, but not healthy teeth. Collectively, we show that the duration of periodontal disease is correlated with increased osteonecrosis and the oral microbiota plays a protective role in ligature-induced osteonecrosis development.

The dissertation of Drake Winslow Williams is approved.

Mo K. Kang

Tara Aghaloo

Yousang Gwack

Reuben H. Kim, Committee Chair

University of California, Los Angeles

2019

DEDICATION

I would like to thank my advisor, Reuben Kim for his support during the past decade. I have learned so much about the academic process from him, from how to read and analyze papers, to performing experiments, writing grants and manuscripts, and presenting my work.

I would also like to thank my committee members for their valuable insights, suggestions, and flexibility. First, I'd like to thank Mo Kang, who was a co-sponsor of my F30 grant. He has always given valuable feedback of my work and has supported my applications whenever asked. Tara Aghaloo is an expert in both the clinical and basic science aspects of MRONJ who has always made a genuine effort to visit my poster presentations and discuss my career aspirations; she is a vital member of my committee. Yousang Gwack has directed me to pursue the immunologic aspects of MRONJ described in Chapter 2, and his advice yielded some very interesting results. I would like to reiterate my gratitude to each of my committee members Reuben Kim, Mo Kang, Tara Aghaloo and Yousang Gwack.

I have been a part of the School of Dentistry community for some time and there are so many people to thank who encouraged my scientific curiosity. I would like to thank Ki-Hyuk Shin, who has always welcomed me and made me feel like a part of a lab family. I would also like to thank No-Hee Park for his support and critical career advice during a difficult time in my dental school training. David Wong has been one of my strongest allies at the School of Dentistry, and words cannot describe how thankful I am for his never-ending support of my scholarship, grant, and clinical fellowship applications. Sotirios Tetradis has given me invaluable career advice, including thoughts on career choices and letters of recommendation. I would also like to thank Wen Shi and Cun-Yu Wang, who were both supportive of me when I first joined the DDS/PhD program and applied for my F30 grant.

Over the past 10 years, I have met and worked with many amazing scholars. In no particular order, I'd like to thank Allison Lenon, Katie Ho, Terresa (TK) Kim, Abdullah Alshaikh, Jinsook (Jinny) Suh, Cindy Lee, Shebli (Shebs) Mehrazarin, Sol Kim, Thomas Fung, Wei Chen, Paul Yang, and Rachel Lee. Thank you all for your help, support and encouragement!

None of this would be possible without strong family support. Therefore, I dedicate this work to my biggest supporters: Helen, my mom, dad and sister, and (this) man's best friend, Bertie.

TABLE OF CONTENTS

ACKNOWLEDGEMENTS

My graduate studies and part of this work was funded by the National Institute of Dental and Craniofacial Research, a branch of the National Institutes of Health (Grant: F30DE025172).

CURRICULUM VITA

EDUCATION

University of California, Los Angeles
B.S. in Microbiology, Immunology and Molecular Genetics — 2012

School of Dentistry, University of California, Los Angeles
Doctor of Dental Surgery (DDS) — 2017

CREDENTIALS

Dental Board of California Dental License, #DDS102119 — 2017 – Present

APPOINTMENTS

Clinical Instructor, Restorative Dentistry, UCLA School of Dentistry — 2017 – Present

RESEARCH SUPPORT

NIDCR/NIH
F30DE025172 — Feb 2015 – Jun 2019
Role: PI
Mentor: Reuben Kim, Mo Kang

PROFESSIONAL SERVICE

Journal of Bone and Mineral Research – *ad hoc* reviewer
Oral Diseases – *ad hoc* reviewer

SELECTED HONORS & AWARDS (EXTRAMURAL BOLDED)

Dentsply Sirona Research Award, ADA Foundation	**2018 - 2019**
Young Investigator Award for PhD Training, ASBMR	**2018**
Henry M. Thornton Fellowship, AADR/SCADA/Dentsply Sirona	**2018**
UCLA Representative, NIDCR Workshop	**2017**
Robert C. Caldwell Research Award, UCLA School of Dentistry	2017
Fred Herzberg Memorial Award, UCLA School of Dentistry	2017
Section of Oral Biology Award, UCLA School of Dentistry	2017
Dean's Leadership Institute (Certificate), UCLA School of Dentistry	2017
Ruth L. Kirschstein National Research Service Award, NIDCR/NIH	**2015 – 2019**
Student Research Fellowship, AADR	**2015 – 2017**
David & Miki Lee Scholarship, UCLA School of Dentistry	2015 – 2016
UCLA Representative, SCADA	**2015**
Johnson & Johnson Hatton Award, AADR	**2015**
Bloc Research Travel Grant, AADR/NIDCR	**2015**
TL1 Science Fellowship, UCLA CTSI	2014
Kathy & Randy Wall Scholarship, UCLA School of Dentistry	2013 – 2017

REFEREED MANUSCRIPTS

1. Kim RH, Lee RS, **Williams D**, Bae S, Woo J, Lieberman M, Oh JE, Dong QH, Shin KH, Kang MK, Park NH. Bisphosphonate induces senescence in normal human oral keratinocytes. J Dent. Res. 2011;90: 810-816. PMCID3144120.
2. Kim RH, **Williams DW**, Bae S, Lee RS, Oh JE, Mehrazarin S, Kim T, Shin KH, Park NH, Kang MK. Camphorquinone inhibits odontogenic differentiation of dental pulp cells and triggers release of inflammatory cytokines. J Endod. 2013 Jan;39(1):57-61. PMCID23228258
3. **Williams DW**, Wu H, Oh JE, Fakhar C, Kang MK, Shin KH, Park NH, Kim RH. HEMA inhibits the migration of dental pulp mesenchymal cells. J Endod. 2013 Sept:39(9):1156-1160. PMCID23953290
4. **Williams DW**, Lee C, Kim T, Yagita H, Wu H, Park S, Yang P, Liu H, Shi S, Shin KH, Kang MK, Park NH, Kim RK. Impaired bone resorption and woven bone formation are associated with development of osteonecrosis of the jaw-like lesions by bisphosphonate and anti-RANKL antibody in mice. Am J Pathol. 2014 Nov;184(11):3084-93. PMCID25173134
5. Pope WH, Bowman CA, Russell DA, Jacobs-Sera D, Asai DJ, Cresawn SG, Jacobs WR, Hendrix RW, Lawrence JG, Hatfull GF, Science Education Alliance Phage Hunters Advancing Genomics and Evolutionary Science, **Phage Hunters Integrating Research and Education (PHIRE)**, and Mycobacterial Genetics Course. Whole genome comparison of a large collection of mycobacteriophages reveals a continuum of phage genetic diversity. eLife. 2015;4:e06416
6. Kim RH, Kang, M, Kim, T, Yang P, Bae S, **Williams DW**, Phung S, Shin K-H, Hong CH, and Park N-H. Epigenetic regulation of p53 during replicative senescence in normal human keratinocytes. Aging Cell. 2015 Jul 1.
7. Kim S, **Williams DW**, Lee C, Kim T, Arai A, Shi S, Li X, Shin KH, Kang MK, Park NH, Kim RH. IL-36 Induces Bisphosphonate-Related Osteonecrosis of the Jaw-Like Lesions in Mice by Inhibiting TGF-β-Mediated Collagen Expression. J Bone Miner Res. 2017 Feb;32(2):309-318.
8. Kim T, Kim S, Song M, Lee C, Yagita H, **Williams DW**, Sung EC, Hong C, Shin KH, Kang MK, Park NH, Kim RH. Removal of pre-existing periodontal inflammatory condition before tooth extraction ameliorates MRONJ-like lesion in mice. Am J Pathol. 2018 Oct;188(10):2318-2327.
9. Gaballa J, Dabrian K, …, **Williams D**, Freise A, and Parker JM. Genome Sequences of Cluster K Mycobacteriophages Deby, LaterM, LilPharaoh, Paola, SgtBeansprout, and Sulley. Genome Announc. Microbiol Resour Announc. 2019 Jan; 8(2): e01481-18.

Chapter 1

Introduction

The oral cavity is a unique and important anatomic site in the human body that harbors dentition required for prandial nutrient extraction, accommodates a diverse commensal microbiota, and is the first site where food antigens are encountered prior to entering the GI tract. The sequela of a disruption in any of these facets of the oral cavity includes decreased quality of life, poor nutrient extraction, commensal microbiota dysbiosis and opportunistic infection, bacteremia and/or septicemia, and in the case of incompatible antigen encounter, anaphylaxis and death. Medication-related osteonecrosis of the jaw (MRONJ) is a nonhealing wound involving epithelium, connective tissue and bone that is unique to the oral-maxillofacial region and significantly alters quality of life. MRONJ is clinically defined as exposed necrotic bone and unclosed overlaying oral mucosa for at least 8 weeks in patients with a history of antiresorptive or antiangiogenic therapy who have not experienced radiation therapy in the maxillofacial region (Ruggiero et al., 2014). It occurs in the mandible and/or maxilla of patients taking antiresorptive or antiangiogenic medicaments for bone degenerative diseases such as osteoporosis or as an adjunctive therapy to minimize cancerous bone metastases. The multifactorial etiology of MRONJ has led to an incomplete understanding of disease pathogenesis since the first cases were reported in 2003 (Marx, 2003).

The goal of this body of work was to understand the etiologic factors that spark MRONJ lesion development by utilizing clinically relevant mouse models. Since only a subset of patients and mice on antiresorptive therapy (ART) develop MRONJ lesions, we compared animals that did or did not develop MRONJ. Treatment group stratification led to the observation that impaired bone resorption and woven bone formation are hallmarks of MRONJ lesions. Additionally, we identified and described a critical role for pro-inflammatory cytokines including interleukin 36 (IL36) in the development of MRONJ that has potential therapeutic utility. Subsequent studies isolated the role of chronic periodontal inflammation and the commensal microbiota in MRONJ lesion development. The tissue-specific nature of MRONJ requires specialized study of the

unique features of the oral barrier and the interplay between barrier structure and function, wound healing, and host-microbiota interactions.

The Oral Barrier: Structure and Function

The human body contains several mucosal tissues that are strategically located in areas that have the potential to encounter external pathogens or insults, including the skin, GI tract, and the oral cavity. Maintenance of tissue homeostasis requires a delicate balance between immune surveillance and response at barrier tissues: too great a response can severely damage the host, while anergic responses can lead to barrier penetration and systemic infection (Belkaid and Harrison, 2017). In addition to efficient recruitment and maintenance of local innate and adaptive immune populations, barrier tissues rely on physical characteristics to maintain their integrity. The oral mucosa is generally comprised of an outer layer of stratified squamous epithelium and an inner layer of dense connective tissue, often referred to as the lamina propria (Winning and Townsend, 2000). Within the oral cavity, there are specific location-dependent modifications to the mucosa which correspond to the primary function of the tissue. The masticatory mucosa of the gingiva and hard palate are modified to have a mechanically tough epithelial covering that consists of a basal layer with undifferentiated epithelial cells, a granular layer with membrane-coating granules that contribute to barrier impermeability, and a highly keratinized layer that resists damage from mastication. The lining mucosa of the lips, cheeks, vestibule, inferior tongue and floor of mouth is non-keratinized enabling distension at the cost of increased susceptibility to physical damage. Specialized mucosa on the dorsal tongue consists of a mixture of keratinized papillae and non-keratinized interpapillary regions (Winning and Townsend, 2000).

One unique anatomic feature of the oral cavity is the dentogingival junction, which is the interface between the tooth and gingiva. The dentogingival junction is the weakest part of the oral barrier due to the connection between mucosa and teeth, called the junctional epithelium,

that lacks tight junctions and is therefore susceptible to pathogen infiltration (Bosshardt and Lang, 2005). Indeed, the niche located directly adjacent to the dentogingival junction is colonized by commensal bacteria that, if allowed to accumulate, can become pathobionts and cause local inflammation leading to a host-mediated destruction of alveolar bone in a process clinically known as periodontitis (Darveau, 2010).

Periodontal Disease

Periodontitis is a chronic, slowly progressing infectious and inflammatory disease that compromises oral barrier integrity at the site of the dentogingival junction. Historically, it was believed that periodontal disease was caused by a group of bacteria called the red complex (*Porphyomonas gingivalis*, *Tannerella forsythia*, and *Treponema denticola*) based on their association with severe periodontal disease (Socransky et al., 1998). However, advances in metagenome and transcriptome sequencing as well as mechanistic studies have enabled a better understanding of the periodontitis-associated microbiome which supports a new model of polymicrobial synergy and dysbiosis. In this model, disease results from an imbalance in the oral flora, where multiple species work in concert to develop a pathogenic environment that leads to destructive host responses. Microbial immune subversion by keystone pathogens is a central feature of this model, and may explain why host response is varied across populations (Hajishengallis, 2015). Clinically, periodontitis is preceded by gingivitis, which is a mild and reversible form of periodontal disease characterized by inflamed gingiva, pseudopocket formation and bleeding, with little to no discomfort and no alveolar bone loss. Left untreated, gingivitis can advance to periodontitis, which is characterized by supra/subgingival plaque accumulation, progressive attachment loss, and alveolar bone loss and may eventually necessitate tooth removal (Fig. 1A, Klokkevold et al., 2018).

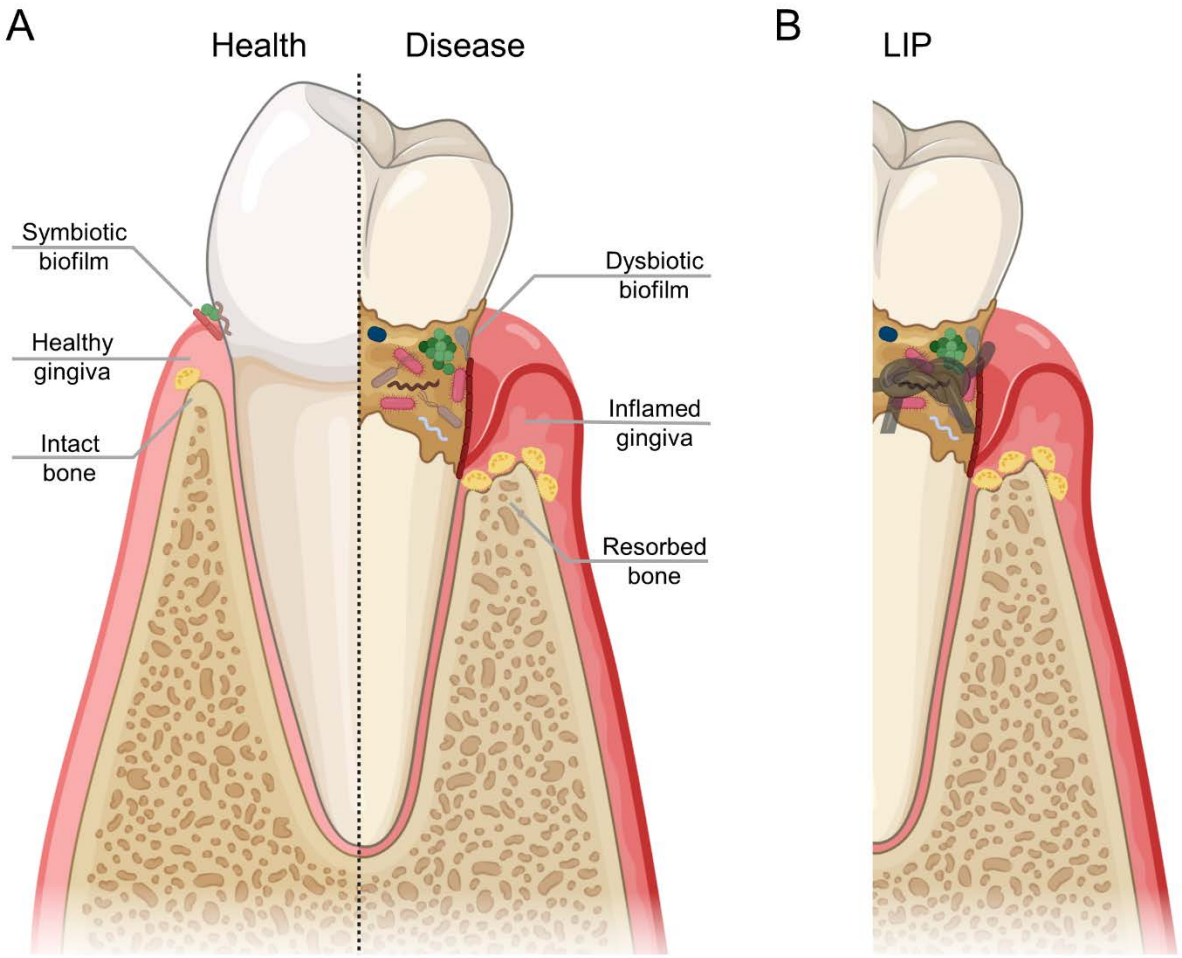

Figure 1. Visual representation of osteomucosal tissue in periodontal disease.

A. In periodontal health (left), biofilm made of symbiotic bacteria colonize the surface of the tooth adjacent to the gingiva. The gingiva is pink, stippled and does not bleed when probed with a dull instrument. Although there is a basal bone homeostasis, there is no appreciable bone resorption. In periodontal disease (right), the community composition of the bacterial biofilm changes if bacterial aggregation is not removed by dental hygiene practices. The biofilm supports the growth of pathobionts, which elicit host responses that include gingival inflammation and an increase in bone resorption by osteoclasts. B. Placement of a suture at the cemento-enamel junction is an artificial method to induce periodontitis in rodents (called ligature-induced periodontitis, LIP).

The study of periodontal disease has been active for over 60 years and has involved human subjects as well as a plethora of mammalian model organisms. As a result, several animal models have been developed to replicate periodontal disease pathogenesis. The ligature model is technically challenging but effective at inducing inflammation and periodontal bone loss by enabling accumulation of dental plaque and micro-ulceration at the dentogingival junction, which facilitates pathogen invasion into the connective tissue (Figure 1B, Graves et al., 2012). Chapters 2 and 3 of this work utilize the ligature model to study the role of short- and long-term ligature placement and understand the role of the commensal microbiota in MRONJ pathogenesis, respectively. Infection models utilizing known amounts of individual bacteria delivered in food also mimic the pathologic bone loss and inflammation associated with periodontal disease (Li et al., 2010). Similarly, introduction of human strains of periodontal pathogens by oral gavage has proven effective at inducing an immune response comparable to that seen in humans (Bainbridge et al., 2010). Finally, local injection of the gram-negative bacterial cell wall component lipopolysaccharide into gingival tissue enables the study of innate immune response in periodontal disease pathogenesis (Buduneli et al., 2007). Each of these models has inherent limitations, but they also enable the study of discrete components of periodontal disease pathology.

Oral Mucosal Wound Healing

In any barrier tissue, expedient resolution of barrier integrity following exogenous insult is critical. Compared to the nuanced barrier defect at the dentogingival junction in periodontal disease, an acute trauma such as a tooth extraction results in a notable barrier defect that is resolved by wound healing. This multi-step and interconnected process requires communication between the gingival epithelium, connective tissue and the bone. The normal response to injury involves 3 overlapping but distinct phases: activation of inflammation, *de novo* tissue formation, and tissue remodeling (Gurtner et al., 2008). Immediately following injury, components of the coagulation cascade are activated, inflammation-related genes are upregulated, and innate

immune cells are recruited in order to stop blood loss and prevent infections. Once a clot is formed by platelets and hemostasis is achieved, a fibrin matrix is formed which acts as the scaffold upon which tissue formation occurs (Grose and Werner, 2004).

The second major phase of extraction socket healing begins with epithelial closure. This orchestrated process starts when basal epithelial cells alter their phenotype to closely resemble a migrating mesenchymal cell (Odland and Ross, 1968). Basal epithelial cells then proliferate and migrate across the wound bed, reverting back to their polarized cell phenotype to assist in the regeneration of the basement membrane (Larjava et al., 2011). Another essential response in the granulation tissue formation process is angiogenesis, as the blood is a major source of nutrients for new cells that are generated during granulation tissue formation (Carmeliet, 2003). Epithelial cell expansion described above occurs concurrently with myofibroblast and stromal progenitor cell proliferation in order to initiate the tissue regeneration phase (Pretheeban et al., 2012). Site-specific soluble signals that originate from epithelial cells, fibroblasts, salivary gland cells, vascular endothelial cells, and nerve cells drive myofibroblast and stromal progenitor cell differentiation, migration, and proliferation (Smith and Martínez, 2018). Once myofibroblasts and stromal cells migrate to the wound bed, they proliferate and rapidly produce extracellular matrix components including collagen, which is mediated by transforming growth factor β1 (Schrementi et al., 2008; Klass et al., 2009). Previously we identified woven bone formation as a distinct feature absent in MRONJ-like lesions (Williams et al., 2014) and we showed that collagen deposition by gingival mesenchymal stem cells is critical in MRONJ pathogenesis due to its role as a scaffold for woven bone formation (Kim et al., 2017).

The final phase in extraction socket healing is tissue remodeling, whereby unorganized extracellular matrix proteins are degraded by matrix metalloproteinases and replaced at a much slower rate to return the tissue to a state that closely resembles uninjured tissue (Gurtner et al., 2008). Importantly, the cells involved in rapid tissue formation (myofibroblasts and stromal cells)

undergo apoptosis to make room for fibroblasts which secrete extracellular matrix components at a slower pace (Desmoulière et al., 1995; Zhang et al., 2004). Finally, inflammation associated genes and cells including macrophages are subdued to reduce the development of scar tissue (Mak et al., 2009).

Medication-Related Osteonecrosis of the Jaw: Overview

Bisphosphonates (BP) are anti-resorptive drugs commonly prescribed to treat bone disorders like osteoporosis and recently they have been utilized in the treatment of bone metastases in cancer patients (Drake et al., 2008). A side effect of anti-resorptive drugs like BPs is that long-term users are at higher risk of developing osteonecrosis of the jaw (ONJ), clinically defined as exposed necrotic bone and unclosed overlaying oral mucosa for at least 8 weeks (Ruggiero et al., 2014). Nitrogen containing bisphosphonates, which include the most recent, most potent, and currently used generation of bisphosphonates, act by disrupting the enzymatic activity of farnesyl pyrophosphate synthase. FPPS is a key regulatory enzyme in the mevalonate pathway that ultimately leads to the production of steroids, cholesterol, and post-translational protein prenylation. In osteoclasts, this is especially important because BPs inhibit the isoprenylation of proteins such as Rho, Rac and Rab. These proteins are critical in forming the ruffled border characteristic of active osteoclasts and without proper post-translational modification, osteoclasts undergo apoptosis (Drake et al., 2008). Denosumab is a monoclonal antibody targeting RANKL, which is a required co-factor for terminal osteoclast differentiation. Thus, when Denosumab binds to RANKL, RANKL can no longer bind to its receptor on osteoclast precursors and no new mature osteoclasts are made (Bridgeman and Pathak, 2011). Although the mechanism of action for BP and Denosumab are diverse, they both cause MRONJ suggesting that ONJ pathogenesis is likely due to inhibition of common cellular processes rather than a drug-specific effect. Furthermore, a completely different class of drugs targeting angiogenesis have also been shown to play a causal role in ONJ development, and consequently, the current naming scheme for this condition was changed to a more broad

"medication" related osteonecrosis of the jaw (MRONJ) in 2014 (Ruggiero et al., 2014). The first report of MRONJ in the literature comes from a case detailed by Marx, who identified 36 patients that developed "painful exposed avascular bone" following nitrogen-bisphosphonate treatment (Marx, 2003). In a letter to the editor, Marx aptly identified that 78% of these patients developed this condition following a tooth extraction. Since then, the bone phenotype now known as MRONJ, has been extensively studied in numerous clinical trials involving bisphosphonates (Lyles et al., 2007; Grbic et al., 2008; McClung et al., 2009; Grbic et al., 2010; Boonen et al., 2012; Sambrook et al., 2012) and denosumab (Fizazi et al., 2011; Henry et al., 2011; Scagliotti et al., 2012; Smith et al., 2012; Chawla et al., 2013; Henry et al., 2014).

In addition to inhibiting osteoclast resorption and stalling the progression of bone degenerative diseases such as osteoporosis and Paget's disease, anti-resorptive drugs have proven effective for cancer therapy which has led to an increase in dosing regimen and the total patient pool that are at risk for developing MRONJ. Cumulative incidence of MRONJ for patients taking intravenous (IV) BPs or Dmab for cancer is approximately the same, conservatively estimated at around 1%, and occurs in approximately 0.1% of patients taking oral bisphosphonates for osteoporosis and other bone degenerative diseases (Ruggiero et al., 2014).

MRONJ Pathogenesis Hypotheses

The pathogenesis of MRONJ thus far appears to be multifactorial, and a number of empirically based hypotheses have emerged to explain its etiology. There are five leading areas of research focus on MRONJ pathogenesis: 1) inhibition of bone remodeling, 2) inflammation and microbial infection, 3) altered immune response, 4) soft tissue toxicity, and 5) angiogenesis inhibition (Aghaloo et al., 2015; Chang et al., 2018).

Bone Remodeling Inhibition

Given that all medications currently known to cause MRONJ have either a direct or indirect effect on bone resorption, a logical MRONJ pathophysiology theory would include altered bone

remodeling. The incorporation of BPs into bone is directly proportional to the local rate of bone turnover (Cremers and Papapoulos, 2011), and increased mechanical load experienced by the jaws during mastication coupled with increased collagen content compared to long bones contribute to a higher rate of bone turnover in the jaws (Sasaki et al., 2010). Interestingly, a study using a fluorescently labeled BP showed that sites with increased bone turnover including extraction sockets and areas with periapical inflammation incorporate increased amounts of BP (Cheong et al., 2014). Additionally, we have previously reported that impaired bone resorption is associated with MRONJ lesions in mice (Williams et al., 2014). Taken together, there is strong evidence that supports that bone remodeling inhibition is central in MRONJ development.

Inflammation and Microbial Infection

The fact that only a small percentage of patients taking antiresorptive or antiangiogenic therapy develop MRONJ suggests that there is an intrinsic factor that, when combined with antiresorptive therapy, leads to MRONJ development. As early as 2005, Marx reported a number of co-factors that were observed in patients who developed MRONJ, including tooth extraction, advanced periodontitis, abscessed teeth, root canal therapy and dental caries, all of which have microbial etiology (Marx et al., 2005). Since then, we and others have shown that dental infection combined with antiresorptive therapy is sufficient to induce murine osteonecrosis in both tooth extraction and non-extraction models (Aghaloo et al., 2011; Cheong et al., 2014; Song et al., 2016; Kim et al., 2018). Adult teeth are typically extracted when the tooth supporting structures are deficient or if the tooth itself is irreparably damaged, and in Chapter 2 we explore how the duration of periodontal inflammation influences the development of osteonecrosis.

Altered Immune Response

The immune system is a critical factor in bone loss and bone regulation, and there is continued debate on the role of innate and adaptive immunity in MRONJ pathogenesis. αβ-T cells are well known to direct pathologic bone loss, but recent studies have shown that a small population of T

cells with the γδ-T cell receptor produce factors that inhibit osteoclast formation and resorptive activity *in vitro* (Pappalardo and Thompson, 2013). Interestingly, this population of γδ-T cells is lost in patients taking bisphosphonates, suggesting a possible role for these cells in helping to reduce disease occurrence (Kalyan et al., 2013). Another study reported slightly more osteonecrosis development in BP-treated wild-type animals compared to γδ-T cell null mice and noted enhanced wound closure by γδ-T cell null mice, suggesting that γδ-T cells may contribute to oral mucosal healing but are unlikely to influence the development of osteonecrosis (Park et al., 2015). In addition to specific cell types that may affect MRONJ pathogenesis, an individual's immune resiliency may determine whether they develop pathology. A group studying MRONJ patients observed a striking correlation between expression of genes related to immune and stress resiliency in peripheral blood leukocytes (including RANK, TNF-α and aryl hydrocarbon receptor) and the oral microbiome composition, which suggests that the microbiome may contribute to host response during MRONJ development (Kalyan et al., 2015), and in Chapter 3 we isolate the role of the commensal microbiota in the development of bone necrosis.

Soft Tissue Toxicity

Prior to the development of α-RANKL antibodies, several groups were interested in the effects of BPs on soft tissue on the basis that some BP may reach the connective tissue or epithelium either from BP ingestion or release of BP during osteoclastic resorption. Indeed, BPs proved to be significantly toxic to cervical, prostate, and oral epithelial cells (Giraudo et al., 2004; Reid et al., 2007; Kim et al., 2011). However, the specificity of the antibody-based antiresorptive treatments and lack of soft tissue toxicity associated with α-RANKL antibody treatment is compelling evidence that toxicity by BPs may modify disease progression but does not drive it.

Angiogenesis Inhibition

A key physiologic feature of necrosis in most tissue types is a lack of blood supply, and an off-target effect of BPs is a reduction in circulating vascular endothelial growth factor which reduces angiogenesis (Wood et al., 2002). Interestingly, the only other class of drugs known to cause

MRONJ are anti-angiogenic agents such as vascular endothelial growth factor inhibitors and tyrosine kinase inhibitors (Estilo et al., 2008; Nicolatou-Galitis et al., 2012). While these drugs are targeted monoclonal antibodies, as a class they have significant untargeted effects on bone metabolism (Alemán et al., 2014). However, normal vasculature was observed in post-mortem MRONJ samples (Hellstein et al., 2011) and α-RANKL antibody treatment has not been associated with vascular changes (Misso et al., 2012). It is likely that angiogenesis inhibition contributes to disease pathogenesis but does not directly cause it.

MRONJ and Periodontal Disease

Periodontitis is one of the most prevalent oral infectious diseases, affecting nearly 50% of the adult population in the United States (Eke et al., 2012; Eke et al., 2015). The connection between periodontitis and MRONJ comes from observational studies, the first of which identified that 84% of patients with clinical MRONJ also suffered from periodontal disease (Marx et al., 2005). Since then, a number of clinical (Boonyapakorn et al., 2008; Ruggiero et al., 2014; Thumbigere-Math et al., 2014) and pre-clinical studies (Aghaloo et al., 2011; Cheong et al., 2014; Song et al., 2016; Kim et al., 2018) have confirmed that periodontal disease is a *bona fide* risk factor for the development of MRONJ. As mentioned in the Periodontitis section above, we utilize the ligature-induced periodontitis (LIP) model to induce local disease that mimics clinical periodontitis in mice. It is clear from our previous studies that necrotic bone formation is increased in diseased teeth following antiresorptive treatment, yet some animals still fail to develop bone necrosis. It is therefore critical to understand the mechanism by which periodontal disease and antiresorptive therapies modify the bone resorption process to enhance necrotic bone formation. In Chapter 2, we investigate and compare the effect of short-term (3 weeks) and long-term (10 weeks) LIP on histologic osteonecrosis, innate and adaptive immune recruitment, and local microbiota composition.

MRONJ and the Oral Microbiota

The extensive body of research that suggested a strong correlation between infectious oral diseases and MRONJ has sparked interest in the potential role of specific pathobionts in osteonecrosis development. A variety of microbial species have been identified from colonies found on excised human MRONJ lesions using scanning electron microscopy (Sedghizadeh et al., 2008) and metagenomic analysis (Pushalkar et al., 2014; Kalyan et al., 2015). Although metagenomic analysis has not consistently revealed an abundance of a particular species, increased *Actinomyces spp.* accumulation on MRONJ lesions has been reported multiple times (Marx et al., 2005; Kaplan et al., 2009; Kos et al., 2010). Moreover, a critical role for bacterial infections in MRONJ pathogenesis has been elucidated by studies showing a decrease in ONJ incidence in cancer patients who improved their oral hygiene (Ripamonti et al., 2009).

Inhibited bone resorption is a central feature in MRONJ development, as osteonecrosis does not occur after treatment with anabolic agents (Hadaya et al., 2019). Interestingly, the commensal microbiota has recently been shown to exert a catabolic effect on bone mass, the mechanism by which is currently under active investigation, but the net effect is increased bone mass in the absence of bacteria (Sjögren et al., 2012; Novince et al., 2017). Additionally, the recommended treatment for MRONJ involves systemic and oral antibiotic treatment in order to reduce infections that may exacerbate symptoms (Ruggiero et al., 2014). Given how critical bone remodeling is during MRONJ pathogenesis, Chapter 3 examines the role of the commensal microbiota in osteonecrosis development following significant reduction in local microbe populations by antibiotic treatment.

Aims

Although the research community has been aware of MRONJ for the past 15 years, there are no targeted treatment methods for MRONJ nor are there reliable detection methods for identifying patients at the highest risk for MRONJ because the exact etiology of the condition is still unclear. The objective of this work was to understand MRONJ pathophysiology in the context of inflammation. In order to do so, we characterized the role of periodontal inflammation and the commensal microbiota on MRONJ pathogenesis.

Aim 1: *To investigate the effect of long-term LIP on MRONJ pathogenesis.* We examined local and systemic differences in bone loss and cytokine expression, respectively, in short-term LIP (S-LIP) and long-term (L-LIP) mouse models. We also utilized 16S sequencing to determine changes in alpha and beta diversity of oral microbiota in S-LIP and L-LIP. Finally, we combined S-LIP and L-LIP with BP treatment and assessed local histologic markers of MRONJ. This work is outlined in Chapter 2 and has not been published.

Aim 2: *To determine the etiologic role of the oral microbiota in MRONJ development.* We established a “germ-reduced” mouse model using broad spectrum antibiotic oral gavage. We determined whether empty lacunae and necrotic bone are altered at the site of tooth extraction in germ-reduced compared to antibiotic-naïve mice treated with BP. We assessed the role of the commensal microbiota in the pathologic bone loss seen in S-LIP. Finally, we assessed the role of the microbiota in inflammation induced MRONJ. This work is outlined in Chapter 3 and has not been published.

References

Aghaloo TL, Kang B, Sung EC, Shoff M, Ronconi M, Gotcher JE, et al. (2011). Periodontal disease and bisphosphonates induce osteonecrosis of the jaws in the rat. *J. Bone Miner. Res.* 26:1871–1882.

Alemán JO, Farooki A, Girotra M (2014). Effects of tyrosine kinase inhibition on bone metabolism: untargeted consequences of targeted therapies. *Endocr. Relat. Cancer* 21:R247–59.

Bainbridge B, Verma RK, Eastman C, Yehia B, Rivera M, Moffatt C, et al. (2010). Role of Porphyromonas gingivalis phosphoserine phosphatase enzyme SerB in inflammation, immune response, and induction of alveolar bone resorption in rats. *Infect. Immun.* 78:4560–4569.

Belkaid Y, Harrison OJ (2017). Homeostatic immunity and the microbiota. *Immunity* 46:562–576.

Boonen S, Reginster J-Y, Kaufman J-M, Lippuner K, Zanchetta J, Langdahl B, et al. (2012). Fracture risk and zoledronic acid therapy in men with osteoporosis. *N. Engl. J. Med.* 367:1714–1723.

Boonyapakorn T, Schirmer I, Reichart PA, Sturm I, Massenkeil G (2008). Bisphosphonate-induced osteonecrosis of the jaws: prospective study of 80 patients with multiple myeloma and other malignancies. *Oral Oncol* 44:857–869.

Bosshardt DD, Lang NP (2005). The junctional epithelium: from health to disease. *J. Dent. Res.* 84:9–20.

Buduneli E, Vardar-Şengül S, Buduneli N, Atilla G, Wahlgren J, Sorsa T (2007). Matrix Metalloproteinases, Tissue Inhibitor of Matrix Metalloproteinase-1, and Laminin-5 γ2 Chain Immunolocalization in Gingival Tissue of Endotoxin-Induced Periodontitis in Rats: Effects of Low-Dose Doxycycline and Alendronate. *J. Periodontol.* 78:127–134.

Carmeliet P (2003). Angiogenesis in health and disease. *Nat. Med.* 9:653–660.

Chawla S, Henshaw R, Seeger L, Choy E, Blay J-Y, Ferrari S, et al. (2013). Safety and efficacy of denosumab for adults and skeletally mature adolescents with giant cell tumour of bone: interim analysis of an open-label, parallel-group, phase 2 study. *Lancet Oncol.* 14:901–908.

Cheong S, Sun S, Kang B, Bezouglaia O, Elashoff D, McKenna CE, et al. (2014). Bisphosphonate uptake in areas of tooth extraction or periapical disease. *J. Oral Maxillofac. Surg.* 72:2461–2468.

Cremers S, Papapoulos S (2011). Pharmacology of bisphosphonates. *Bone* 49:42–49.

Darveau RP (2010). Periodontitis: a polymicrobial disruption of host homeostasis. *Nat. Rev. Microbiol.* 8:481–490.

Desmoulière A, Redard M, Darby I, Gabbiani G (1995). Apoptosis mediates the decrease in cellularity during the transition between granulation tissue and scar. *Am. J. Pathol.* 146:56–66.

Drake MT, Clarke BL, Khosla S (2008). Bisphosphonates: mechanism of action and role in clinical practice. *Mayo Clin. Proc.* 83:1032–1045.

Eke PI, Dye BA, Wei L, Slade GD, Thornton-Evans GO, Borgnakke WS, et al. (2015). Update on Prevalence of Periodontitis in Adults in the United States: NHANES 2009 to 2012. *J. Periodontol.* 86:611–622.

Eke PI, Dye BA, Wei L, Thornton-Evans GO, Genco RJ, CDC Periodontal Disease Surveillance workgroup: James Beck (University of North Carolina, Chapel Hill, USA), Gordon Douglass (Past President, American Academy of Periodontology), Roy Page (University of Washin (2012). Prevalence of periodontitis in adults in the United States: 2009 and 2010. *J. Dent. Res.* 91:914–920.

Estilo CL, Fornier M, Farooki A, Carlson D, Bohle G, Huryn JM (2008). Osteonecrosis of the jaw related to bevacizumab. *J. Clin. Oncol.* 26:4037–4038.

Fizazi K, Carducci M, Smith M, Damião R, Brown J, Karsh L, et al. (2011). Denosumab versus zoledronic acid for treatment of bone metastases in men with castration-resistant prostate cancer: a randomised, double-blind study. *Lancet* 377:813–822.

Giraudo E, Inoue M, Hanahan D (2004). An amino-bisphosphonate targets MMP-9-expressing macrophages and angiogenesis to impair cervical carcinogenesis. *J. Clin. Invest.* 114:623–633.

Graves DT, Kang J, Andriankaja O, Wada K, Rossa C (2012). Animal models to study host-bacteria interactions involved in periodontitis. *Front. Oral Biol.* 15:117–132.

Grbic JT, Black DM, Lyles KW, Reid DM, Orwoll E, McClung M, et al. (2010). The incidence of osteonecrosis of the jaw in patients receiving 5 milligrams of zoledronic acid: data from the health outcomes and reduced incidence with zoledronic acid once yearly clinical trials program. *J Am Dent Assoc* 141:1365–1370.

Grbic JT, Landesberg R, Lin S-Q, Mesenbrink P, Reid IR, Leung P-C, et al. (2008). Incidence of osteonecrosis of the jaw in women with postmenopausal osteoporosis in the health outcomes and reduced incidence with zoledronic acid once yearly pivotal fracture trial. *J Am Dent Assoc* 139:32–40.

Grose R, Werner S (2004). Wound-healing studies in transgenic and knockout mice. *Mol. Biotechnol.* 28:147–166.

Gurtner GC, Werner S, Barrandon Y, Longaker MT (2008). Wound repair and regeneration. *Nature* 453:314–321.

Hadaya D, Gkouveris I, Soundia A, Bezouglaia O, Boyce RW, Stolina M, et al. (2019). Clinically Relevant Doses of Sclerostin Antibody Do Not Induce Osteonecrosis of the Jaw (ONJ) in Rats with Experimental Periodontitis. *J. Bone Miner. Res.* 34:171–181.

Hajishengallis G (2015). Periodontitis: from microbial immune subversion to systemic inflammation. *Nat. Rev. Immunol.* 15:30–44.

Hellstein JW, Adler RA, Edwards B, Jacobsen PL, Kalmar JR, Koka S, et al. (2011). Managing the care of patients receiving antiresorptive therapy for prevention and treatment of osteoporosis: executive summary of recommendations from the American Dental Association Council on Scientific Affairs. *J Am Dent Assoc* 142:1243–1251.

Henry D, Vadhan-Raj S, Hirsh V, von Moos R, Hungria V, Costa L, et al. (2014). Delaying skeletal-related events in a randomized phase 3 study of denosumab versus zoledronic acid in patients with advanced cancer: an analysis of data from patients with solid tumors. *Support. Care Cancer* 22:679–687.

Henry DH, Costa L, Goldwasser F, Hirsh V, Hungria V, Prausova J, et al. (2011). Randomized, double-blind study of denosumab versus zoledronic acid in the treatment of bone metastases in patients with advanced cancer (excluding breast and prostate cancer) or multiple myeloma. *J. Clin. Oncol.* 29:1125–1132.

Kalyan S, Quabius ES, Wiltfang J, Mönig H, Kabelitz D (2013). Can peripheral blood γδ T cells predict osteonecrosis of the jaw? An immunological perspective on the adverse drug effects of aminobisphosphonate therapy. *J. Bone Miner. Res.* 28:728–735.

Kalyan S, Wang J, Quabius ES, Huck J, Wiltfang J, Baines JF, et al. (2015). Systemic immunity shapes the oral microbiome and susceptibility to bisphosphonate-associated osteonecrosis of the jaw. *J. Transl. Med.* 13:212.

Kaplan I, Anavi K, Anavi Y, Calderon S, Schwartz-Arad D, Teicher S, et al. (2009). The clinical spectrum of Actinomyces-associated lesions of the oral mucosa and jawbones: correlations with histomorphometric analysis. *Oral Surg. Oral Med. Oral Pathol. Oral Radiol. Endod.* 108:738–746.

Kim RH, Lee RS, Williams D, Bae S, Woo J, Lieberman M, et al. (2011). Bisphosphonates induce senescence in normal human oral keratinocytes. *J. Dent. Res.* 90:810–816.

Kim T, Kim S, Song M, Lee C, Yagita H, Williams DW, et al. (2018). Removal of Pre-Existing Periodontal Inflammatory Condition before Tooth Extraction Ameliorates Medication-Related Osteonecrosis of the Jaw-Like Lesion in Mice. *Am. J. Pathol.* 188:2318–2327.

Klass BR, Grobbelaar AO, Rolfe KJ (2009). Transforming growth factor beta1 signalling, wound healing and repair: a multifunctional cytokine with clinical implications for wound repair, a delicate balance. *Postgrad. Med. J.* 85:9–14.

Klokkevold PR, Newman MG, Takei HH, Carranza FA (2018). Newman and Carranza's Clinical Periodontology.

Kobayashi Y, Udagawa N, Takahashi N (2009). Action of RANKL and OPG for osteoclastogenesis. *Crit. Rev. Eukaryot. Gene Expr.* 19:61–72.

Kos M, Brusco D, Kuebler J, Engelke W (2010). Clinical comparison of patients with osteonecrosis of the jaws, with and without a history of bisphosphonates administration. *Int J Oral Maxillofac Surg* 39:1097–1102.

Larjava H, Koivisto L, Häkkinen L, Heino J (2011). Epithelial integrins with special reference to oral epithelia. *J. Dent. Res.* 90:1367–1376.

Li Y, Messina C, Bendaoud M, Fine DH, Schreiner H, Tsiagbe VK (2010). Adaptive immune response in osteoclastic bone resorption induced by orally administered Aggregatibacter actinomycetemcomitans in a rat model of periodontal disease. *Mol. Oral Microbiol.* 25:275–292.

Lyles KW, Colón-Emeric CS, Magaziner JS, Adachi JD, Pieper CF, Mautalen C, et al. (2007). Zoledronic acid and clinical fractures and mortality after hip fracture. *N. Engl. J. Med.* 357:1799–1809.

Mak K, Manji A, Gallant-Behm C, Wiebe C, Hart DA, Larjava H, et al. (2009). Scarless healing of oral mucosa is characterized by faster resolution of inflammation and control of myofibroblast action compared to skin wounds in the red Duroc pig model. *J. Dermatol. Sci.* 56:168–180.

Marx RE (2003). Pamidronate (Aredia) and zoledronate (Zometa) induced avascular necrosis of the jaws: a growing epidemic. *J. Oral Maxillofac. Surg.* 61:1115–1117.

Marx RE, Sawatari Y, Fortin M, Broumand V (2005). Bisphosphonate-induced exposed bone (osteonecrosis/osteopetrosis) of the jaws: risk factors, recognition, prevention, and treatment. *J. Oral Maxillofac. Surg.* 63:1567–1575.

McClung M, Miller P, Recknor C, Mesenbrink P, Bucci-Rechtweg C, Benhamou C-L (2009). Zoledronic acid for the prevention of bone loss in postmenopausal women with low bone mass: a randomized controlled trial. *Obstet. Gynecol.* 114:999–1007.

Misso G, Porru M, Stoppacciaro A, Castellano M, De Cicco F, Leonetti C, et al. (2012). Evaluation of the in vitro and in vivo antiangiogenic effects of denosumab and zoledronic acid. *Cancer Biol. Ther.* 13:1491–1500.

Nicolatou-Galitis O, Migkou M, Psyrri A, Bamias A, Pectasides D, Economopoulos T, et al. (2012). Gingival bleeding and jaw bone necrosis in patients with metastatic renal cell carcinoma receiving sunitinib: report of 2 cases with clinical implications. *Oral Surg. Oral Med. Oral Pathol. Oral Radiol.* 113:234–238.

Novince CM, Whittow CR, Aartun JD, Hathaway JD, Poulides N, Chavez MB, et al. (2017). Commensal Gut Microbiota Immunomodulatory Actions in Bone Marrow and Liver have Catabolic Effects on Skeletal Homeostasis in Health. *Sci. Rep.* 7:5747.

Odland G, Ross R (1968). Human wound repair. I. Epidermal regeneration. *J. Cell Biol.* 39:135–151.

Pappalardo A, Thompson K (2013). Activated γδ T cells inhibit osteoclast differentiation and resorptive activity in vitro. *Clin. Exp. Immunol.* 174:281–291.

Park S, Kanayama K, Kaur K, Tseng H-CH, Banankhah S, Quje DT, et al. (2015). Osteonecrosis of the jaw developed in mice: DISEASE VARIANTS REGULATED BY γδ T CELLS IN ORAL MUCOSAL BARRIER IMMUNITY. *J. Biol. Chem.* 290:17349–17366.

Pretheeban T, Lemos DR, Paylor B, Zhang R-H, Rossi FM (2012). Role of stem/progenitor cells in reparative disorders. *Fibrogenesis Tissue Repair* 5:20.

Pushalkar S, Li X, Kurago Z, Ramanathapuram LV, Matsumura S, Fleisher KE, et al. (2014). Oral microbiota and host innate immune response in bisphosphonate-related osteonecrosis of the jaw. *Int. J. Oral Sci.* 6:219–226.

Reid IR, Bolland MJ, Grey AB (2007). Is bisphosphonate-associated osteonecrosis of the jaw caused by soft tissue toxicity? *Bone* 41:318–320.

Ripamonti CI, Maniezzo M, Campa T, Fagnoni E, Brunelli C, Saibene G, et al. (2009). Decreased occurrence of osteonecrosis of the jaw after implementation of dental preventive measures in solid tumour patients with bone metastases treated with bisphosphonates. The experience of the National Cancer Institute of Milan. *Ann. Oncol.* 20:137–145.

Ruggiero SL, Dodson TB, Fantasia J, Goodday R, Aghaloo T, Mehrotra B, et al. (2014). American Association of Oral and Maxillofacial Surgeons position paper on medication-related osteonecrosis of the jaw--2014 update. *J. Oral Maxillofac. Surg.* 72:1938–1956.

Sambrook PN, Roux C, Devogelaer J-P, Saag K, Lau C-S, Reginster J-Y, et al. (2012). Bisphosphonates and glucocorticoid osteoporosis in men: results of a randomized controlled trial comparing zoledronic acid with risedronate. *Bone* 50:289–295.

Sasaki M, Matsuura T, Katafuchi M, Tokutomi K, Sato H (2010). Higher Contents of Mineral and Collagen but Lower of Hydroxylysine of Collagen in Mandibular Bone Compared with Those of Humeral and Femoral Bones in Human. *J. Hard Tissue Biology.* 19:175–180.

Scagliotti GV, Hirsh V, Siena S, Henry DH, Woll PJ, Manegold C, et al. (2012). Overall survival improvement in patients with lung cancer and bone metastases treated with denosumab versus zoledronic acid: subgroup analysis from a randomized phase 3 study. *J. Thorac. Oncol.* 7:1823–1829.

Schrementi ME, Ferreira AM, Zender C, DiPietro LA (2008). Site-specific production of TGF-beta in oral mucosal and cutaneous wounds. *Wound Repair Regen.* 16:80–86.

Sedghizadeh PP, Kumar SKS, Gorur A, Schaudinn C, Shuler CF, Costerton JW (2008). Identification of microbial biofilms in osteonecrosis of the jaws secondary to bisphosphonate therapy. *J. Oral Maxillofac. Surg.* 66:767–775.

Sjögren K, Engdahl C, Henning P, Lerner UH, Tremaroli V, Lagerquist MK, et al. (2012). The gut microbiota regulates bone mass in mice. *J. Bone Miner. Res.* 27:1357–1367.

Smith MR, Saad F, Coleman R, Shore N, Fizazi K, Tombal B, et al. (2012). Denosumab and bone-metastasis-free survival in men with castration-resistant prostate cancer: results of a phase 3, randomised, placebo-controlled trial. *Lancet* 379:39–46.

Smith PC, Martínez C (2018). Wound healing in the oral mucosa. In LA Bergmeier, editor *Oral mucosa in health and disease*. Cham: Springer International Publishing, pp. 77–90.

Socransky SS, Haffajee AD, Cugini MA, Smith C, Kent RL (1998). Microbial complexes in subgingival plaque. *J. Clin. Periodontol.* 25:134–144.

Song M, Alshaikh A, Kim T, Kim S, Dang M, Mehrazarin S, et al. (2016). Preexisting Periapical Inflammatory Condition Exacerbates Tooth Extraction-induced Bisphosphonate-related Osteonecrosis of the Jaw Lesions in Mice. *J Endod* 42:1641–1646.

Thumbigere-Math V, Michalowicz BS, Hodges JS, Tsai ML, Swenson KK, Rockwell L, et al. (2014). Periodontal disease as a risk factor for bisphosphonate-related osteonecrosis of the jaw. *J. Periodontol.* 85:226–233.

Winning TA, Townsend GC (2000). Oral mucosal embryology and histology. *Clin Dermatol* 18:499–511.

Wood J, Bonjean K, Ruetz S, Bellahcène A, Devy L, Foidart JM, et al. (2002). Novel antiangiogenic effects of the bisphosphonate compound zoledronic acid. *J. Pharmacol. Exp. Ther.* 302:1055–1061.

Zhang X, Kohli M, Zhou Q, Graves DT, Amar S (2004). Short- and long-term effects of IL-1 and TNF antagonists on periodontal wound healing. *J. Immunol.* 173:3514–3523.

Chapter 2

Long-term ligature-induced periodontitis exacerbates MRONJ development in mice*

***In preparation for publication**

Abstract

Medication-related osteonecrosis of the jaw (MRONJ) is a detrimental intraoral lesion that occurs in patients with long-term or high-dose use of anti-resorptive agents such as bisphosphonates (BP). Tooth extractions are known risk factors for MRONJ, and these interventions are often performed to eliminate existing pathological inflammatory conditions. Previously, we determined that ligature-induced periodontitis (LIP) is a risk factor for MRONJ, but it remains unclear whether the chronicity of LIP influences MRONJ development. In this study, we assess the effect of LIP (for 3 or 10 weeks) on MRONJ development. We analyzed alveolar bone loss in maxillae using μCT. We harvested maxillary oral mucosal tissue and analyzed pro- and anti-inflammatory cytokine expression by quantitative real-time PCR. Systemic pro-inflammatory cytokine levels were assessed by ELISA. Hallmarks of ONJ, innate and adaptive immune populations were quantified from histologic sections. Although systemic BP treatment prevented alveolar bone loss induced by 10-week ligature placement, when a diseased tooth was extracted in mice with BP administration, histologic hallmarks of MRONJ including empty lacunae and necrotic bone increased compared to the group receiving BP and extraction of a healthy tooth. We also observed significant increases in PF4 and MIP1γ in mice that received BP treatment and had tooth extractions compared to controls. Additionally, we identify CD3+ T cells as the major immune population in both health and disease and observe a significant increase in CD4+IL23R+ T cells in MRONJ-like lesions. Taken together, our study reveals that extracting a periodontally compromised tooth increases the formation of necrotic bone compared to extracting a periodontally healthy tooth.

Introduction

Antiresorptive therapy with bisphosphonates such as zoledronic acid (ZOL) is the current front-line therapy for bone degenerative diseases such as osteoporosis (Compston et al., 2019). Additionally, bisphosphonates are becoming an increasingly important tool in reducing bone pain and skeletal related events in metastatic bone disease (Neville-Webbe and Coleman, 2010). Nitrogen containing bisphosphonates including ZOL act by inhibiting post-translational prenylation of proteins critical for osteoclast function, ultimately leading to osteoclast apoptosis and inhibition of osteoclast-mediated bone resorption (Roelofs et al., 2006).

A rare but detrimental side effect of bisphosphonates is the development of medication related osteonecrosis of the jaw (MRONJ), which often occurs at the site of a tooth extraction or invasive dental surgery (Kennel and Drake, 2009). The pathophysiology of MRONJ has been extensively studied since the first report in 2003 (Marx, 2003) but remains elusive to date (Aghaloo et al., 2015). Notable current hypotheses to explain MRONJ development include bone remodeling inhibition (Williams et al., 2014), inflammation and infection (Aghaloo et al., 2011; Kim et al., 2018), angiogenesis inhibition (Lescaille et al., 2014), soft tissue toxicity (Kim et al., 2011), and innate or acquired immune dysfunction (Kikuiri et al., 2010).

While several risk factors for MRONJ development have been reported in the literature, many reported MRONJ cases occur following the extraction of a tooth with local pathologic inflammation (Thumbigere-Math et al., 2014). This clinical observation has been corroborated in several animal models of periodontal and periapical disease with concomitant antiresorptive treatment and tooth extraction (Song et al., 2016; Kim et al., 2018; Aghaloo et al., 2011; Soundia et al., 2018). These studies have established that localized periodontal inflammation is a *bona fide* risk factor for MRONJ development.

Periodontal inflammation increases necrotic bone formation compared to antiresorptive treatment alone in animal studies. Thus, advancing our understanding of how periodontal

inflammation leads to an increase in necrotic bone formation during antiresorptive treatment is of critical clinical importance. In the following study, we investigate and compare the effect of short-term (3 weeks) and long-term (10 weeks) ligature induced periodontitis (S-LIP and L-LIP, respectively) on histologic osteonecrosis, innate and adaptive immune recruitment, and local microbiota composition.

Materials and Methods

Animals

6-week-old female C57BL/6J mice were purchased from the Jackson Laboratories and housed in a specific pathogen free environment with 12-hour light/dark cycle managed by the UCLA Division of Laboratory and Animal Medicine. All experimental protocols were approved by institutional guidelines from the Chancellor's Animal Research Committee (2011-062).

Ligature-induced periodontitis mouse models

We have modified our previously established mouse model for MRONJ (Williams et al., 2014) to include varying times of ligature-induced inflammation preceding the tooth extraction and healing phase. To summarize, mice were subjected to either short- or long-term (3 or 10 weeks, respectively) ligature-induced periodontitis (LIP) without any anti-resorptive intervention (**Figure 1A**), where a 6-0 suture was placed around the second maxillary molar (M2) under general anesthesia as described previously (Kim et al., 2018). A separate cohort of mice were subjected to long-term LIP (L-LIP) while undergoing biweekly intravenous infusions of 0.9% NaCl (Veh) or Zoledronic Acid (ZOL; 125μg/kg; Sagent Pharmaceuticals) (**Figure 3A**). A third cohort of mice underwent L-LIP and ZOL treatment followed by M2 extraction and healing for three weeks (**Figure 4A**). A final cohort of mice underwent either short-term LIP (S-LIP) or L-LIP and ZOL treatment followed by M2 extraction and healing for three weeks (**Appendix Figure 5A**).

Micro-computed tomography and bone loss analysis

Whole maxillae were scanned with a voxel size of $10\mu m^3$ using a 1.0 mm aluminum filter at 60 kVp and 166μA (SkyScan 1275; Bruker). Other scanning parameters include rotation step of 0.4 degrees, frame averaging of 6 and random movement. 2-dimensional images were reconstructed using N Recon (Bruker) following X-Y alignment and dynamic range adjustment. Reconstructed images were saved as 16-bit TIFF images and used for bone loss analysis. Bone loss was quantified by measuring the distance between cementoenamel junction and the alveolar ridge on the palatal, mesiobuccal and distobuccal roots of M2 using CTAn (Bruker). 3-dimensional representative images were generated in CTVox (Bruker).

Histomorphometric and histochemical staining

We evaluated histologic signs of MRONJ lesions by hematoxylin and eosin staining following decalcification and paraffin embedding as described previously without modification (Williams et al., 2014). We determined the number of Tartrate-resistant acid phosphatase-positive osteoclasts around the M2 region with a kit according to the manufacturer's protocol (#387A-1KT, Millipore Sigma).

Immunofluorescence staining

Formalin fixed paraffin embedded tissues were rehydrated by serial dilutions of xylene and ethanol. Antigen retrieval in citrate buffer was carried out at 60°C overnight. Sections were blocked in 10% normal goat serum and incubated in primary antibody diluted in 3% serum overnight at 4°C. Primary antibodies included CD3 (#ab5690, Abcam), CD19 (#ab25232, Abcam), CD66b (#ab197678, Abcam), F4/80 (#MCA497GA, Bio-Rad), CD4 (#12-0041-83, Thermofisher Scientific), and IL23R (#ab53656, Abcam). After washing, secondary antibody diluted in 3% serum was incubated for 1 hour followed by DAPI counterstain for 8 minutes. Slides were mounted using Prolong Gold (P36930; Thermofisher Scientific) and imaged with a confocal microscope (LSM700; Zeiss).

Multiplexed sandwich ELISA Array

We assayed sera from S-LIP and L-LIP animals with and without ZOL treatment to determine changes in 40 different pro-inflammatory cytokines following the manufacturer's protocol (#QAM-CYT-5; RayBiotech). Glass slides were imaged by RayBiotech and raw data was extracted and analyzed in Excel.

Quantitative real-time PCR

To assess local changes in inflammatory cytokines, palatal tissues immediately adjacent to the ligated M2 were processed to obtain RNA as described and cDNA using qScript cDNA SuperMix following manufacturer's protocol (#101414-108; VWR). Gene expression was assessed using PowerUp SYBR Green Master Mix (#100029284; Applied Biosystems) in a QuantStudio 3 Real-Time PCR System (Applied Biosystems). Fold differences between

samples were calculated with the ΔΔCt method using 18S as the housekeeping gene. Primer sequences can be found in Table 1.

Table 1. List of primers

Gene	Forward (5'-3')	Reverse (5'-3')	Species
18S	GTAACCCGTTGAACCCCATT	CCATCCAATCGGTAGTAGCG	Mouse
Tnf	CCCTCACACTCAGATCATCTTCT	GCTACGACGTGGGCTACAG	Mouse
Il1b	GCAACTGTTCCTGAACTCAACT	ATCTTTTGGGGTCCGTCAACT	Mouse
Il6	TAGTCCTTCCTACCCCAATTTCC	TTGGTCCTTAGCCACTCCTTC	Mouse
Il10	GCTCTTACTGACTGGCATGAG	CGCAGCTCTAGGAGCATGTG	Mouse
Tgfb1	CTCCCGTGGCTTCTAGTGC	GCCTTAGTTTGGACAGGATCTG	Mouse
Igf1	CTGGACCAGAGACCCTTTGC	GGACGGGGACTTCTGAGTCTT	Mouse
Foxp3	CCCATCCCCAGGAGTCTTG	ACCATGACTAGGGGCACTGTA	Mouse
Il17a	TTTAACTCCCTTGGCGCAAAA	CTTTCCCTCCGCATTGACAC	Mouse
Mmp9	ACGACATAGACGGCATCCA	GCTGTGGTTCAGTTGTGGTG	Mouse

16S rRNA Sequencing

Bacterial DNA was extracted from fecal, oral, spleen and liver samples as described above. Library preparation was performed as described (Tong et al., 2014) using uniquely barcoded primers targeting the V4 region of the 16S gene (Caporaso et al., 2012). Pooled libraries diluted to 6pM in 20% PhiX underwent paired-end (2x250bp) sequencing using the Illumina MiSeq v2 platform. Demultiplexed sequencing results were analyzed with the QIIME pipeline (Caporaso et al., 2010).

Statistical Analysis

All data are shown as mean ± SEM. For all figures, differences between groups were compared by one- or two-way ANOVA with Tukey's post-hoc test, as appropriate. *$p < 0.05$; **$p < 0.01$; ***$p < 0.001$; ****$p < 0.0001$; ns, not statistically significant.

Results

Long-term ligature placement exacerbates bone loss and pro-inflammatory cytokine expression

To determine the effect of prolonged ligature treatment in mice, we compared local consequences of S-LIP and L-LIP (**Fig. 1A**). Gross photographic examination revealed an increase in blanched areas surrounding L-LIP sites compared to S-LIP and no-ligature control (NLC) sites (**Appendix Fig. 1A**). µCT analysis showed a marked increase in the area of bone resorption at L-LIP sites compared to S-LIP (**Appendix Fig. 1B**). As previously reported, cemento-enamel junction (CEJ) to alveolar bone crest (ABC) distance was significantly increased in S-LIP compared to NLC sites (Kim et al., 2018), but L-LIP resulted in even further CEJ-ABC distance compared to S-LIP (**Fig. 1B-C**). Histologic analysis revealed increased inflammatory infiltrate and bone loss at the site of ligature placement that was accompanied by a significant increase in osteoclast number (**Fig. 1D-E, Appendix Fig. 1C**). No changes were observed in bone loss, osteoclast number, or gross histology between NLC sites in S-LIP and L-LIP, so all NLC samples were combined during analysis. Previous reports have suggested that ligature placement elicits a systemic immune response that is both gender and time dependent (Bain et al., 2009; Saadi-Thiers et al., 2013), so we assessed pro-inflammatory cytokine expression in serum using a multiplex cytokine array. We observed a non-statistically significant increase in cytokines such as IL1β, IL6, and IL17 in LIP groups compared to the control, but no differences were observed in a time-dependent manner (**Appendix Fig. 2**). In contrast, chemokines PF4 and MIP1γ were significantly increased after ligature treatment compared to controls (**Fig. 1F**). Liver *Igf1* and *Tgf-β* increased in a time-dependent manner, whereas in the gingiva, only *Il17a* expression was significantly increased in L-LIP animals compared to S-LIP and NLC groups (**Fig 1G, Appendix Fig. 1D-F**). Together, this proof-of-concept animal model establishes a clear difference in bone loss and cyto/chemokine expression in short- and long-term LIP.

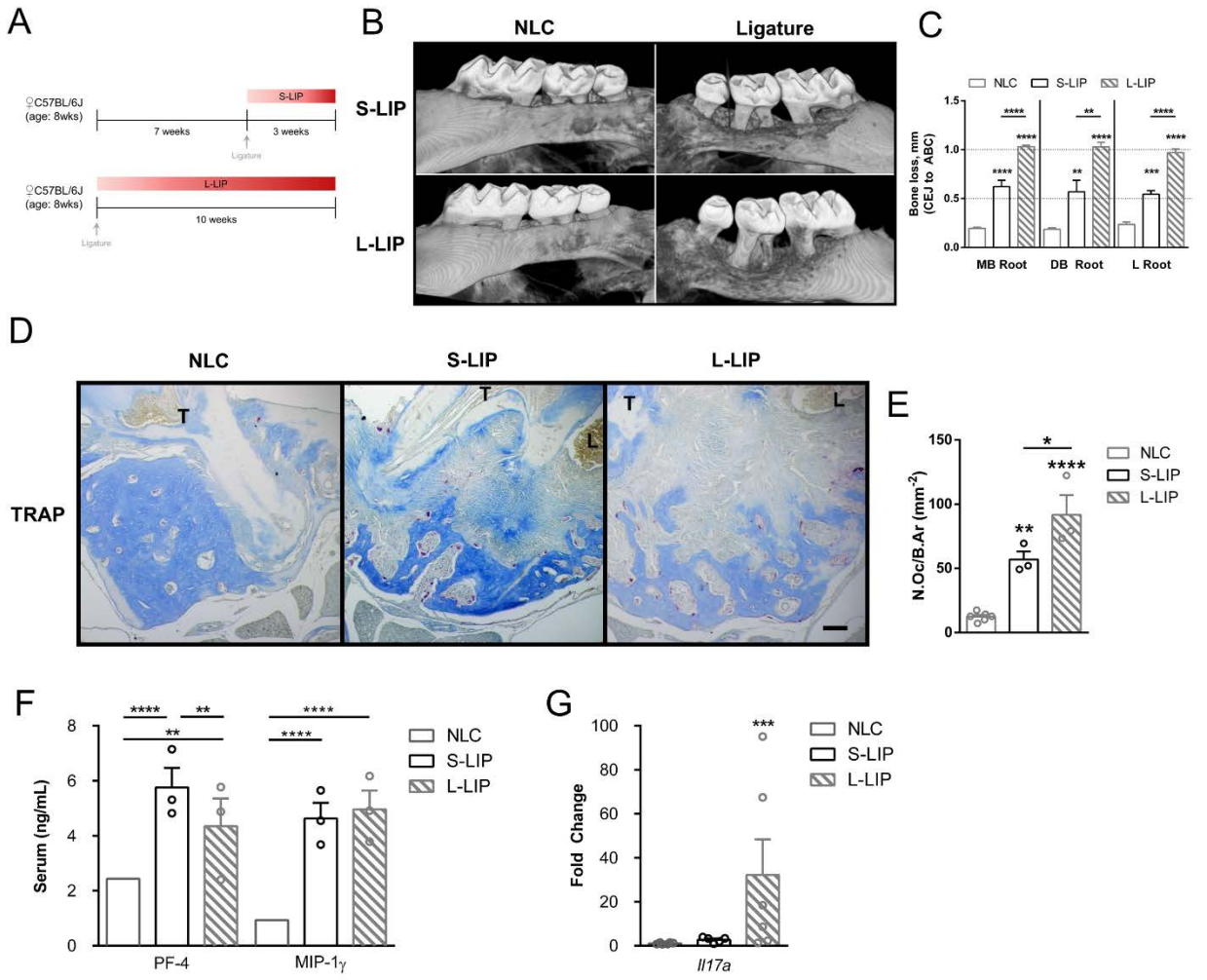

Figure 1. Phenotypic characterization of short- and long-term ligature induced periodontitis.
A. Visual representation of the experimental timeline. Briefly, 8-week-old C57BL/6J mice were split into two groups. The first group received no treatment for 7 weeks, and then a 6-0 silk suture was tied around the second maxillary molar. The second group received the suture for 10 weeks. B. Saggital view of μCT scanned and reconstructed maxilla depicting buccal bone loss at ligature and no-ligature control sites in S-LIP and L-LIP mice. No differences were seen between NLC from S-LIP and L-LIP samples, so these sites were combined into a single 'NLC' group for analysis. C. Quantification of bone loss at each of the second maxillary molar roots. D. TRAP staining on coronal histologic sections at the site of ligation. Tooth (T) and ligature (L) are labeled for reference. Bar: 100μm. E. Quantification of TRAP-positive multinucleated osteoclasts at the site of ligature placement. F. Serum analysis of pro-inflammatory cytokine array targets platelet factor 4 (PF-4) and macrophage inflammatory factor 1 gamma (MIP-1γ). G. Quantitative real-time PCR of gingival tissue taken from ligature or no-ligature control sites. S-LIP, short-term ligature-induced periodontitis (3 weeks); L-LIP, long-term ligature-induced periodontitis (10 weeks), NLC, no-ligature

control; MB, mesio-buccal; DB, disto-buccal; L (root), lingual; N.Oc/B.Ar, number of osteoclasts per bone area. *p<0.05; **p<0.01; ***p<0.001; ****p<0.0001. Data is presented as mean ± SEM.

Host response drives pathologic bone loss in L-LIP

In the LIP mouse model, the ligature supports microbe aggregation at the dentogingival junction which enables microbe invasion into the connective tissue (Graves et al., 2012). Given the significant differences in pathologies between S-LIP and L-LIP, we aimed to understand whether this was due to altered microbe composition on the ligature or an extended host response to inflammation. 16S sequencing revealed significantly reduced alpha and beta diversity at the amplicon sequence variant level on S- and L-LIP ligatures compared to controls, but no differences were seen in diversity metrics between S-LIP and L-LIP alone (**Fig. 2A-C**), suggesting that there are no differences between the number and type of microbes on LIP ligatures after 3 or 10 weeks. To understand how differences in the length of ligature placement affect local immune responses, we stained coronal sections at the site of ligature placement with surface markers for T cells, B cells, tissue resident macrophages and granulocytes (**Fig. 2D, Appendix Fig. 3**). Both CD3+ T cells and F4/80+ macrophages significantly increased in a time dependent manner, whereas CD66b+ granulocytes increased in S-LIP but not in L-LIP (**Fig. 2E**). CD19+ B cells were undetected in the samples tested (not shown). The total number of immune cells per treatment condition were tallied to reveal that CD3+ T cells were the dominant immune cell in both health and disease (**Fig. 2F**). These data suggest that host response rather than microbiota composition is primarily responsible for pathologic bone loss seen in LIP.

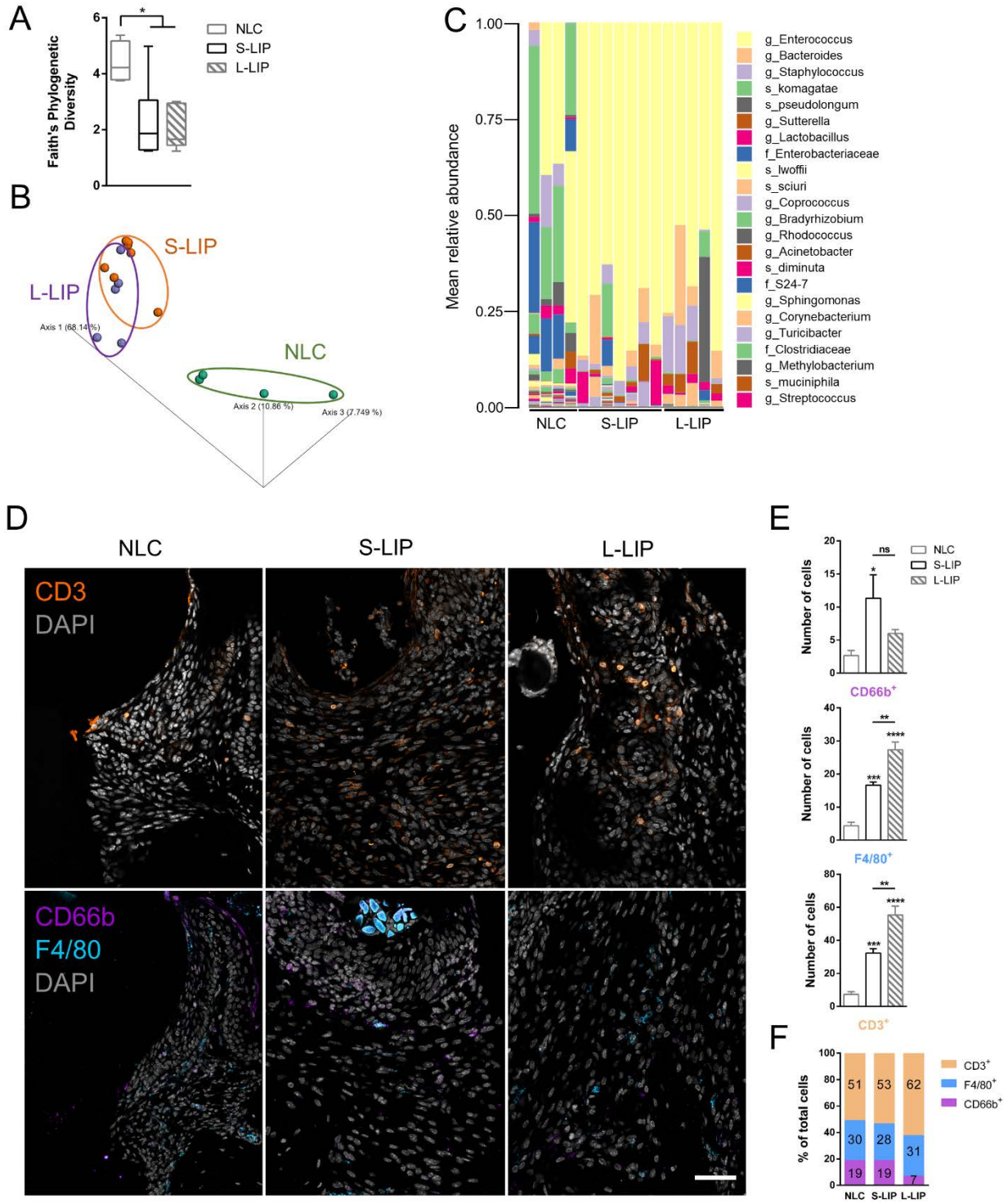

Figure 2. Host response drives pathologic bone loss in LIP.

A,B. The alpha (A) and beta (B) diversity of the microbial communities found at the site of ligature placement were calculated by Faith's phylogenetic diversity and Bray-Curtis dissimilarity principal component analysis, respectively.

C. Microbiome composition is shown at the amplicon sequence variant level (ASV). The top 23 ASVs are classified at

the highest taxonomic level identified. s_, species; g_, genus; f_, family. D-F. Representative images and quantification of immunofluorescent staining at the site of ligature placement. The total number of cells (E) were counted and the proportion of each cell type present was tallied (F). Scale bar: 50μm. S-LIP, short-term ligature-induced periodontitis (3 weeks); L-LIP, long-term ligature-induced periodontitis (10 weeks), NLC, no-ligature control; *p<0.05; **p<0.01; ***p<0.001; ****p<0.0001. Data is presented as mean ± SEM.

L-LIP and BP treatment in combination induce osteonecrosis in mice

Although clinical MRONJ typically occurs after a tooth extraction or dental surgery, rat studies have suggested that osteonecrosis develops in the presence of periodontal disease without tooth extraction (Aghaloo et al., 2011; Li et al., 2016). To determine the effect of concomitant L-LIP and BP treatment on bone resorption and osteonecrosis development we treated a cohort of mice with combinations of L-LIP and/or BP (**Fig. 3A**). Gross examination of maxillae after 10 weeks revealed significant epithelial recession at vehicle (Veh) treated LIP sites that was not present in BP treated LIP or NLC sites (**Appendix Fig. 4A, left**). μCT analysis showed a marked reduction in the palatal extent of bone resorption at L-LIP/ZOL sites compared to L-LIP/Veh sites (**Appendix Fig. 4A, right, black arrowheads**). Sagittal views of μCT reconstructions demonstrated the efficacy of ZOL at inhibiting L-LIP-induced alveolar bone resorption (**Fig 3B,C**). Although we observed no significant difference in bone loss between L-LIP/ZOL and NLC animals, the bone immediately adjacent to the ligature site had a unique appearance compared to NLC sites (**Fig 3B, white arrowheads**). Histologic analysis confirmed that the buccal bone directly adjacent to the ligature site was necrotic, and necrosis was only seen in the L-LIP/ZOL cohort (**Fig 3D,E**). L-LIP treatment resulted in a significant increase in the number of $TRAP^{+}$ osteoclasts regardless of antiresorptive therapy (**Fig 3F,G**). This data cumulatively suggests that osteonecrosis develops independently of tooth extractions in mice following L-LIP treatment.

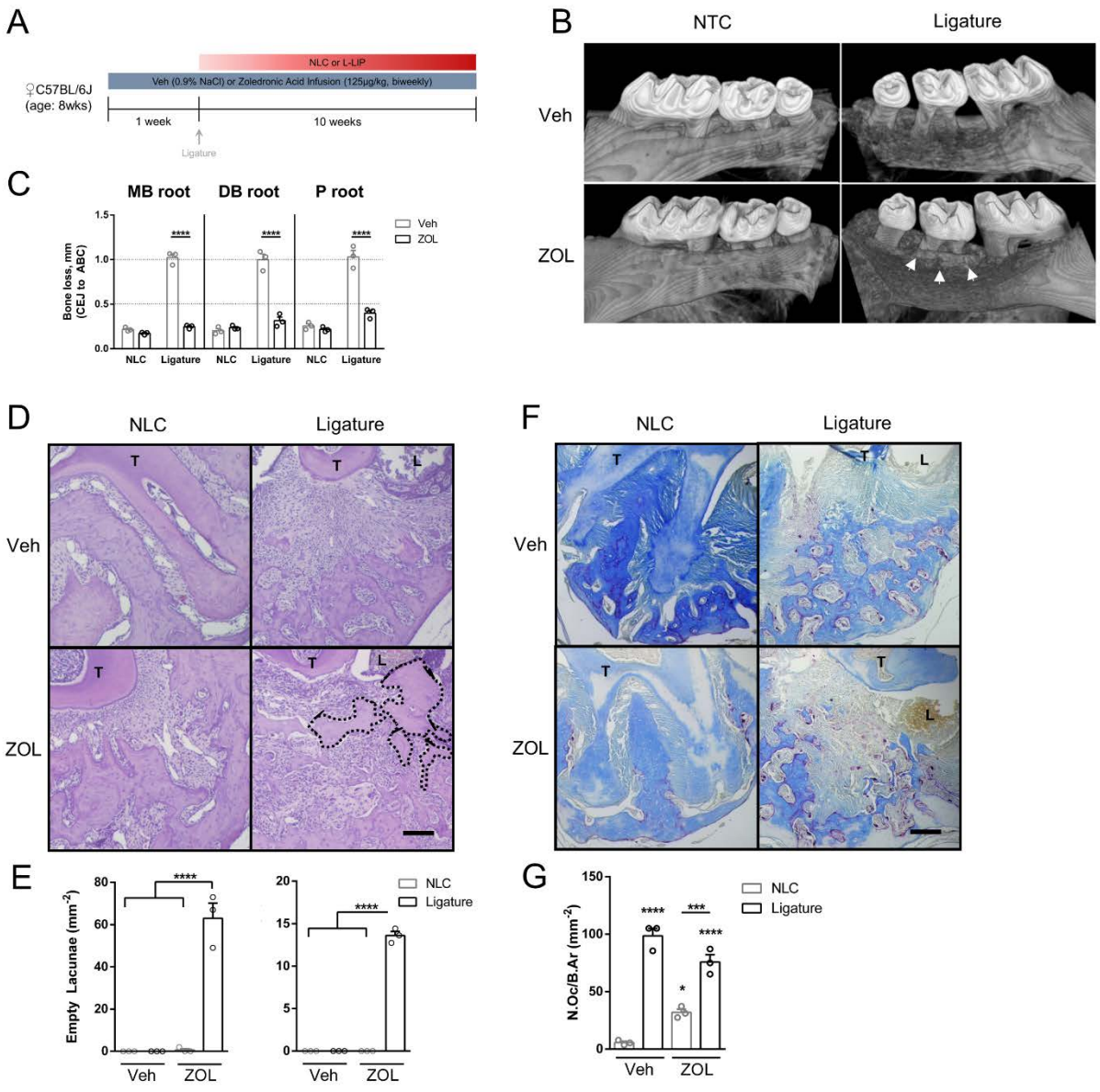

Figure 3. Long-term ligature and anti-resorptive therapy leads to extraction-independent osteonecrosis.
A. 8-week-old C57BL/6 mice were split into two groups. These groups received biweekly intravenous injections of vehicle or zoledronic acid for the entire study. After one week of infusions, half of the mice in each group received a suture as described in Figure 1A for 10 weeks. B. Saggital view of μCT scanned and reconstructed maxilla depicting buccal bone loss. White arrowheads point to necrotic bone at the site of ligature placement visible by μCT. C. Quantification of bone loss at each of the second maxillary molar roots. D. Hematoxylin & Eosin staining on coronal histologic sections at the site of ligation. Tooth (T) and ligature (L) are labeled for reference. Necrotic bone is outlined by the black dotted line. Scale bar: 100μm. E. Quantification of empty lacunae (left) and necrotic bone (right) from histology sections. F. TRAP staining on coronal histologic sections at the site of ligation. Tooth (T) and ligature (L) are

labeled for reference. Scale bar: 100μm. G. Quantification of TRAP-positive multinucleated osteoclasts at the site of ligature placement. Veh, vehicle; ZOL, zoledronic acid; NLC, no-ligature control; MB, mesio-buccal; DB, disto-buccal; P, palatal; N.Oc/B.Ar, number of osteoclasts per bone area. *p<0.05; **p<0.01; ***p<0.001; ****p<0.0001. Data is presented as mean ± SEM.

L-LIP and ZOL induce osteonecrosis development in a tooth extraction mouse model

In our non-extraction L-LIP/ZOL mouse model we observed significant osteonecrosis development in the L-LIP/ZOL group but none in the NLC/ZOL group (**Fig 3B-E**). To isolate the role of tooth extraction and L-LIP in osteonecrosis pathogenesis, we observed bone phenotypes in mice treated with BP and/or L-LIP, where the ligatured tooth was extracted and underwent healing for 3 weeks (**Fig. 4A**). Gross photograph and µCT showed significant inhibition of extraction socket resorption in ZOL treated animals (**Appendix Fig. 4B**). Like L-LIP/ZOL animals without extraction, L-LIP/ZOL with extraction resulted in significant buccal bone necrosis visible by both µCT and histology (**Fig. 4B, white arrows, C-D**). In line with previous findings (Williams et al., 2014; Kim et al., 2018) we observed moderate but significantly less osteonecrosis development in NLC/ZOL compared to L-LIP/ZOL mice (**Fig. 4C-D**). The number of $TRAP^+$ osteoclasts increased in all groups compared to the control, and a trending increase was observed in the number of $TRAP^+$ osteoclasts in NLC/ZOL and L-LIP/ZOL groups (**Fig. 4E-F**). Cumulatively, this data shows the additive effect of ligature-induced inflammation and tooth extraction on osteonecrosis development in mice.

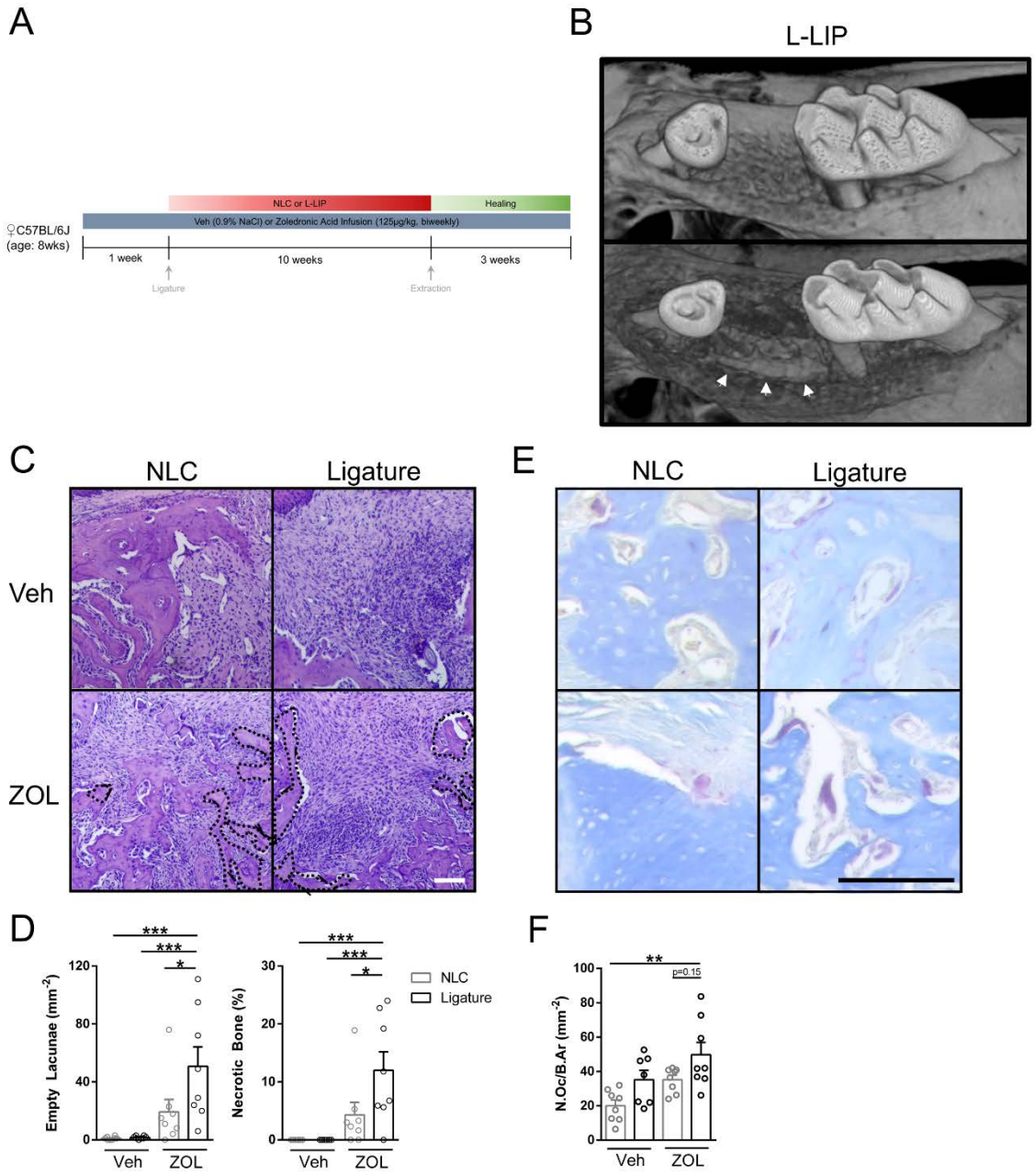

Figure 4. Long-term ligature and anti-resorptive therapy leads to post-extraction osteonecrosis.

A. Mice were divided exactly as in Figure 3A. After 10 weeks of ligature, mice underwent bilateral second maxillary molar extractions and were allowed to heal for 3 weeks prior to sacrifice.B. Clinical (left) and µCT reconstructed photographs (transverse view, middle; saggital view, left) depicting soft tissue healing and extent of socket remodeling. White arrowheads point to necrotic bone at the second maxillary molar visible by µCT. B. Hematoxylin & Eosin staining on coronal histologic sections at the extraction site. Necrotic bone is outlined by the black dotted lines. Scale bar: 100µm. C. Quantification of empty lacunae (left) and necrotic bone (right) from histology sections. D.

TRAP staining on coronal histologic sections at the site of extraction. Scale bar: 100μm. E. Quantification of TRAP-positive multinucleated osteoclasts at the site of extraction. Veh, vehicle; ZOL, zoledronic acid; NLC, no-ligature control; N.Oc/B.Ar, number of osteoclasts per bone area. *p<0.05; **p<0.01; ***p<0.001. Data is presented as mean ± SEM.

Duration of ligature placement is associated with osteonecrosis development in mice

Previous studies have universally identified periodontitis as an important risk factor for the development of osteonecrotic lesions in rodent models and in clinical studies. One caveat to the published rodent studies is that periodontal disease was not allowed to progress to a point where bone loss was substantial enough that would necessitate extraction. To determine whether the duration of ligature placement influences osteonecrosis development in mice, we assessed osteonecrosis development in L-LIP/ZOL and S-LIP/ZOL models (**Appendix Fig. 5A**). Although gross photographs showed similar patterns of epithelial closure between L-LIP and S-LIP groups, μCT analysis confirmed that the bony sequestrum seen in previous L-LIP/ZOL studies was unique to the L-LIP group (**Fig 5A**). Histologic analysis revealed that empty lacunae and percent bone necrosis increased in a ligature duration-dependent manner (**Fig 5B-C**). In contrast to short- and long-term periodontitis models, serum levels of MIP1γ and PF4 increased in a time-dependent manner (**Fig 5D**). We previously found that CD3+ T cell counts increased following LIP in a time-dependent manner (**Fig. 2D-F**). T_h17 cells are a subset of $CD3^+$ T cells and drive the pathologic bone loss in periodontal disease (Dutzan et al., 2018) and have been implicated in a multiple myeloma model of MRONJ (Zhang et al., 2013). We quantified $CD4^+IL23R^+$ cells at the site of ligature placement and found significantly increased numbers in both S-LIP and L-LIP/ZOL samples compared to Veh controls. Interestingly, the increase in $CD4^+IL23R^+$ was confined to S-LIP and L-LIP/ZOL samples that had incomplete epithelial closure in addition to necrotic bone (**Fig. 5E-F**). Together, these findings suggest that duration of periodontal inflammation is critical in MRONJ pathogenesis.

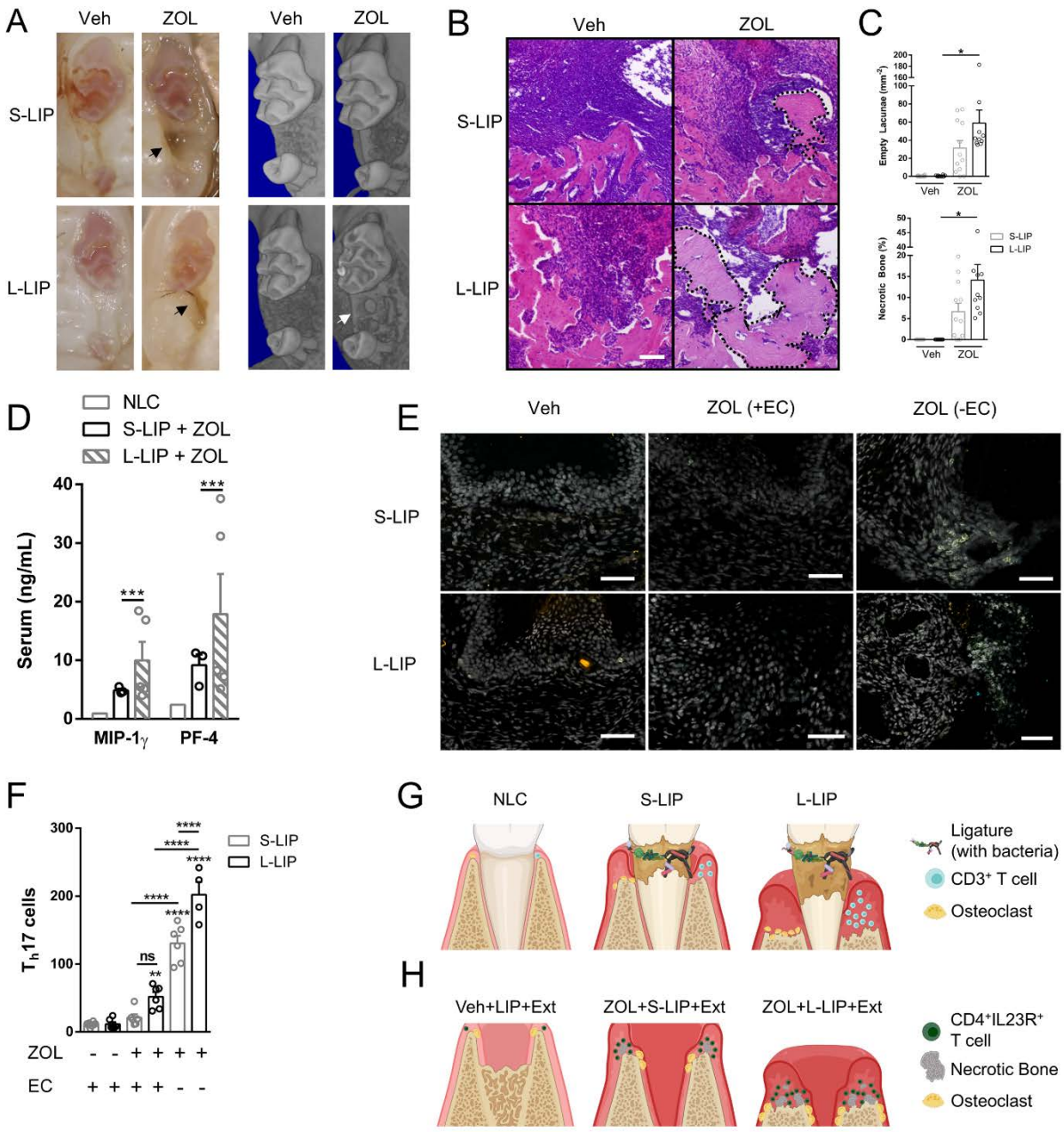

Figure 5. Osteonecrosis development is dependent on duration of ligature-induced periodontitis.
A. Clinical (left) and μCT (right) reconstructed photographs depicting epithelial and osseous healing following extraction. Black arrowheads show exposed bone with incomplete epithelial closure. White arrowhead points to necrotic bone at the site of extraction visible by μCT. B. Hematoxylin & Eosin staining on coronal histologic sections at the site of tooth extraction. Necrotic bone is outlined by the black dotted lines. Scale bar: 100μm. C. Quantification of empty lacunae (left) and necrotic bone (right) from histology sections. D. Serum analysis of pro-inflammatory cytokine array targets platelet factor 4 (PF-4) and macrophage inflammatory factor 1 gamma (MIP-1γ). E,F. Representative images and quantification of dual labeled immunofluorescent staining colocalized to DAPI at the site

of extraction. Scale bar: 50μm. G,H. Summary illustration of findings. (G) In L-LIP, the number of osteoclasts and $CD3^+$ T cells is increased compared to S-LIP, but the number and type of bacteria is the same. (H) When LIP is combined with antiresorptive therapy and extraction, the amount of necrotic bone and number of $CD4^+IL23R^+$ T cells is increased in L-LIP compared to S-LIP. Veh, vehicle; ZOL, zoledronic acid; S-LIP, short-term ligature-induced periodontitis; L-LIP, long-term ligature-induced periodontitis; EC, epithelial closure. *p<0.05; **p<0.01; ***p<0.001; ****p<0.0001. Data is presented as mean ± SEM.

Discussion

In this study, we identify phenotypic characteristics of S-LIP and L-LIP mouse models including differences in alveolar bone loss, osteoclast number, local and systemic expression of pro-inflammatory cytokines, microbiome, and local immune cell populations (**Fig. 1,2**). We show that osteonecrosis develops independently of tooth extractions in the L-LIP model combined with zoledronic acid treatment and consistently forms necrotic bone that is visible by μCT (**Fig. 3,4,5A**). Additionally, we show that the duration of local periodontal inflammation is an important factor in osteonecrosis development, potentially due to heightened Th17 cell recruitment (**Fig. 5**).

Although many confounding variables including genetic background, anti-resorptive dose, age, and others are controlled in animal models of MRONJ, only a percentage of animals develop MRONJ-like lesions. It is therefore critical to develop models that consistently produce the MRONJ-like phenotype in order to minimize the number animals required to obtain relevant results. By inducing long-term inflammation, we have developed a model where almost all animals consistently develop some level of osteonecrosis while at the same time maintaining clinically relevant doses of ZOL (**Fig. 5**). Moreover, our L-LIP treatment results in significant bone loss (**Fig. 1C**), to the point where tooth prognosis is severely compromised which closely mimics a clinical situation that would warrant extraction.

A cytokine array assay detected significantly increased levels of PF4 in S-LIP and L-LIP (**Fig. 1F**). PF4 is stored within platelet α-granules and is released upon inflammation-induced platelet activation (Harrison and Cramer, 1993). A link between platelet activity and periodontitis has been established (Papapanagiotou et al., 2009; Nicu et al., 2009; Al-Rasheed, 2012) and studies have shown increased soluble PF4 in gingival crevicular fluid and serum of patients with severe periodontitis (Greinacher et al., 2011; Brousseau-Nault et al., 2017), suggesting that PF4 may be a biomarker of advanced periodontal disease. PF4 is degraded by matrix metalloproteinase 9 (MMP9) (Van den Steen et al., 2000), which is inhibited by

bisphosphonates like ZOL (Teronen et al., 1999). Assessment of PF4 in our mouse model of L-LIP combined with ZOL therapy and tooth extraction revealed a time-dependent increase in PF4 levels (**Fig. 5D**), presumably due to decreased MMP9-mediated degradation by ZOL. We speculate that PF4 may be used to identify patients taking bisphosphonates that have advanced periodontal disease and are therefore at high risk for developing MRONJ.

Maintenance of barrier integrity is critical for host survival, and this is especially important during periodontal infection and following dentoalveolar surgery. The role of the oral microbiota in MRONJ pathogenesis remains controversial, although a recent study identified that there were no apparent differences in the microbial populations of MRONJ patients compared to healthy controls (Kalyan et al., 2015). Instead, the patients who developed MRONJ had significantly reduced expression of genes that regulate immune and barrier function. The dominating immune population in both health and periodontal disease are $CD3^+$ T cells (**Fig. 2F**, (Dutzan et al., 2016). Interestingly, the number of $CD4^+IL23R^+$ T cells is significantly higher at the extraction site in S-LIP and L-LIP mice treated with ZOL compared to Veh controls, and increases with longer ligature placement periods (**Fig. 5F**). Interestingly, the length of ligature placement did not alter the number or type of microbes that colonized the ligature (**Fig. 2A-C**), suggesting that host response to inflammation plays a larger role than microbiota composition in pathologic bone loss and osteonecrosis development in our mouse model. Overall, further studies are warranted to determine the exact role of T cells in MRONJ pathogenesis.

In summary, we have established and characterized a mouse model of long-term ligature-induced inflammation that leads to the development of osteonecrosis in mice. We have identified that the duration of inflammation is associated with the amount of necrotic bone formation following tooth extraction in mice receiving ZOL infusions. Our study also provides evidence to support clinical guidelines that prioritize the resolution of pathologic inflammatory conditions in ZOL users to reduce the likelihood of MRONJ development.

Appendix

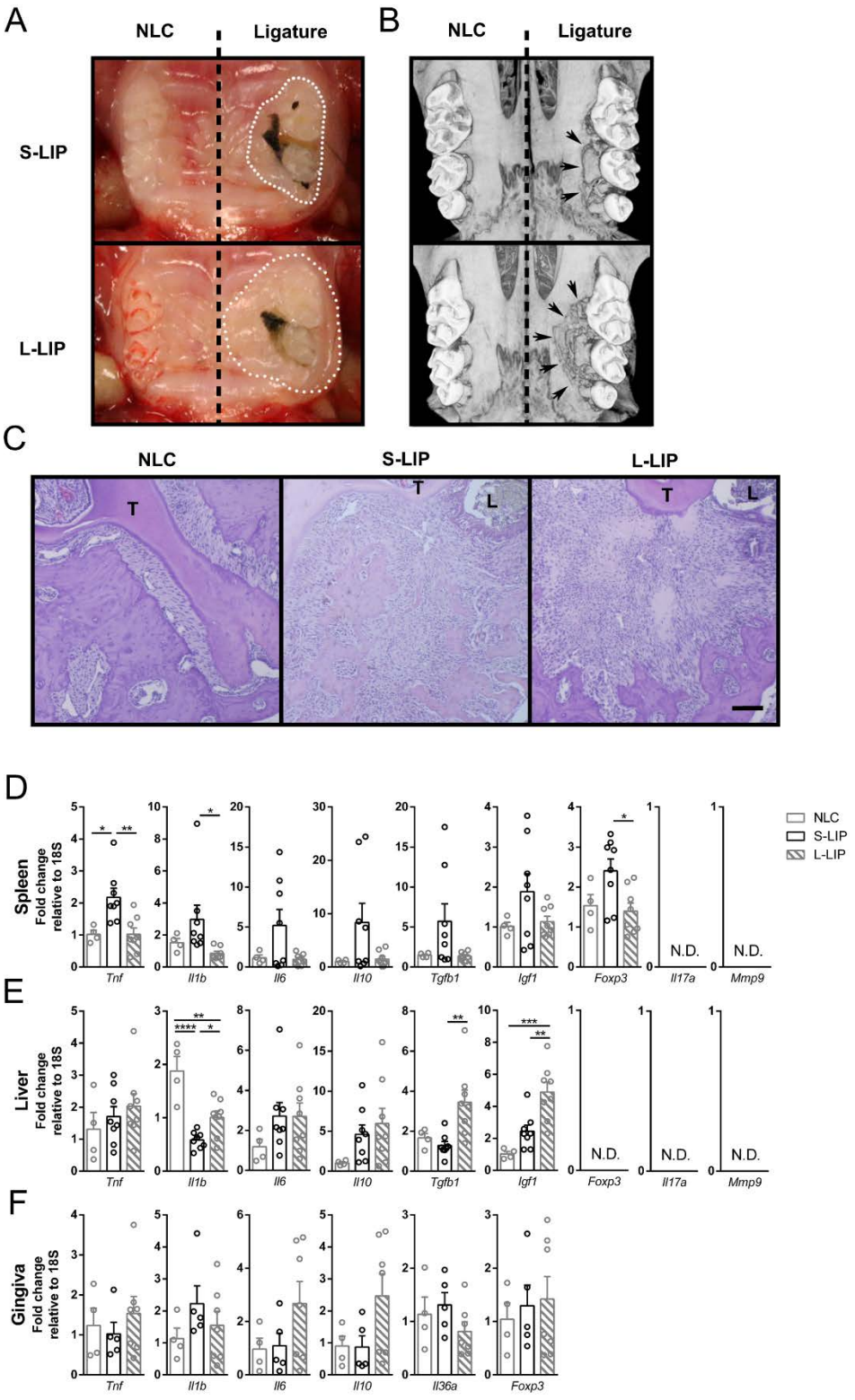
A
NLC
Ligature
S-LIP
L-LIP
B
NLC
Ligature
C
NLC
S-LIP
L-LIP
T
L
D
Spleen
Fold change relative to 18S
Tnf
Il1b
Il6
Il10
Tgfb1
Igf1
Foxp3
Il17a
Mmp9
N.D.
NLC
S-LIP
L-LIP
E
Liver
Fold change relative to 18S
F
Gingiva
Fold change relative to 18S
Il36a

Appendix Figure 1.
A. Clinical photograph depicting ligature and no-ligature control sites in S-LIP and L-LIP mice. White dotted lines depict extent of tissue blanching caused by ligature placement. B. Transverse view of µCT scanned and reconstructed maxilla. Black arrowheads indicate extent of resorption caused by ligature placement. C. Hematoxylin & Eosin staining on coronal histologic sections at the site of ligation showing inflammatory infiltrate at the site of ligature placement. Tooth (T) and ligature (L) are labeled for reference. Bar: 100µm. D-F. Quantitative real-time PCR of spleen (D), liver (E), and gingival tissue taken from ligature or no-ligature control sites (F). S-LIP, short-term ligature-induced periodontitis (3 weeks); L-LIP, long-term ligature-induced periodontitis (10 weeks), NLC, no-ligature control. *p<0.05; **p<0.01; ***p<0.001; ****p<0.0001. Data is presented as mean ± SEM.

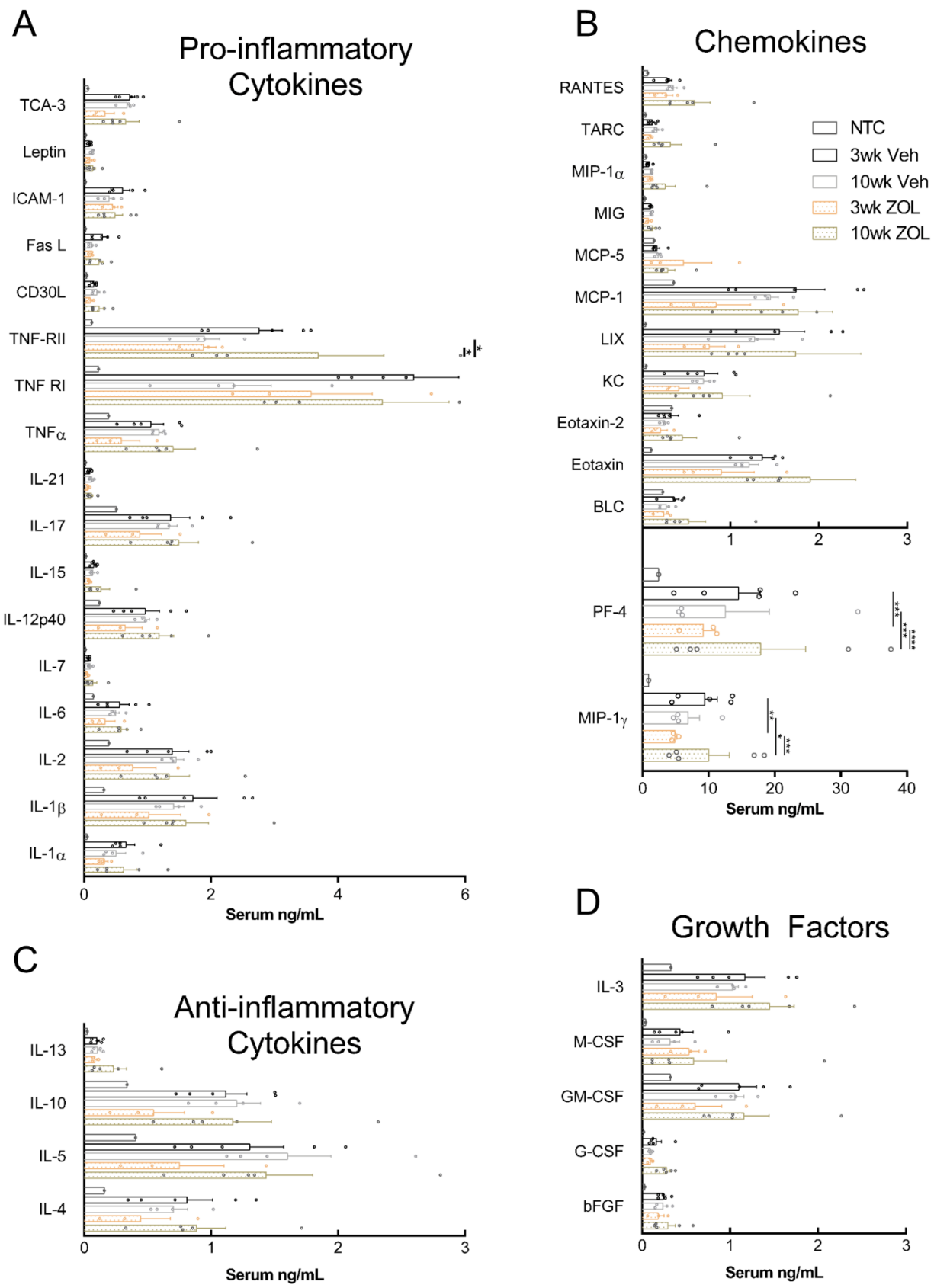
A
Pro-inflammatory Cytokines
TCA-3
Leptin
ICAM-1
Fas L
CD30L
TNF-RII
TNF RI
TNFα
IL-21
IL-17
IL-15
IL-12p40
IL-7
IL-6
IL-2
IL-1β
IL-1α
0
2
4
6
Serum ng/mL
B
Chemokines
RANTES
TARC
MIP-1α
MIG
MCP-5
MCP-1
LIX
KC
Eotaxin-2
Eotaxin
BLC
PF-4
MIP-1γ
NTC
3wk Veh
10wk Veh
3wk ZOL
10wk ZOL
1
2
3
0
10
20
30
40
Serum ng/mL
C
Anti-inflammatory Cytokines
IL-13
IL-10
IL-5
IL-4
0
1
2
3
Serum ng/mL
D
Growth Factors
IL-3
M-CSF
GM-CSF
G-CSF
bFGF
0
1
2
3
Serum ng/mL

Appendix Figure 2.
Serum analysis of pro-inflammatory cytokine array targets are shown. Targets are separated by general function including pro-inflammatory cytokines (A), chemokines (B), anti-inflammatory cytokines (C), and growth factors (D). *p<0.05; ***p<0.001; ****p<0.0001.

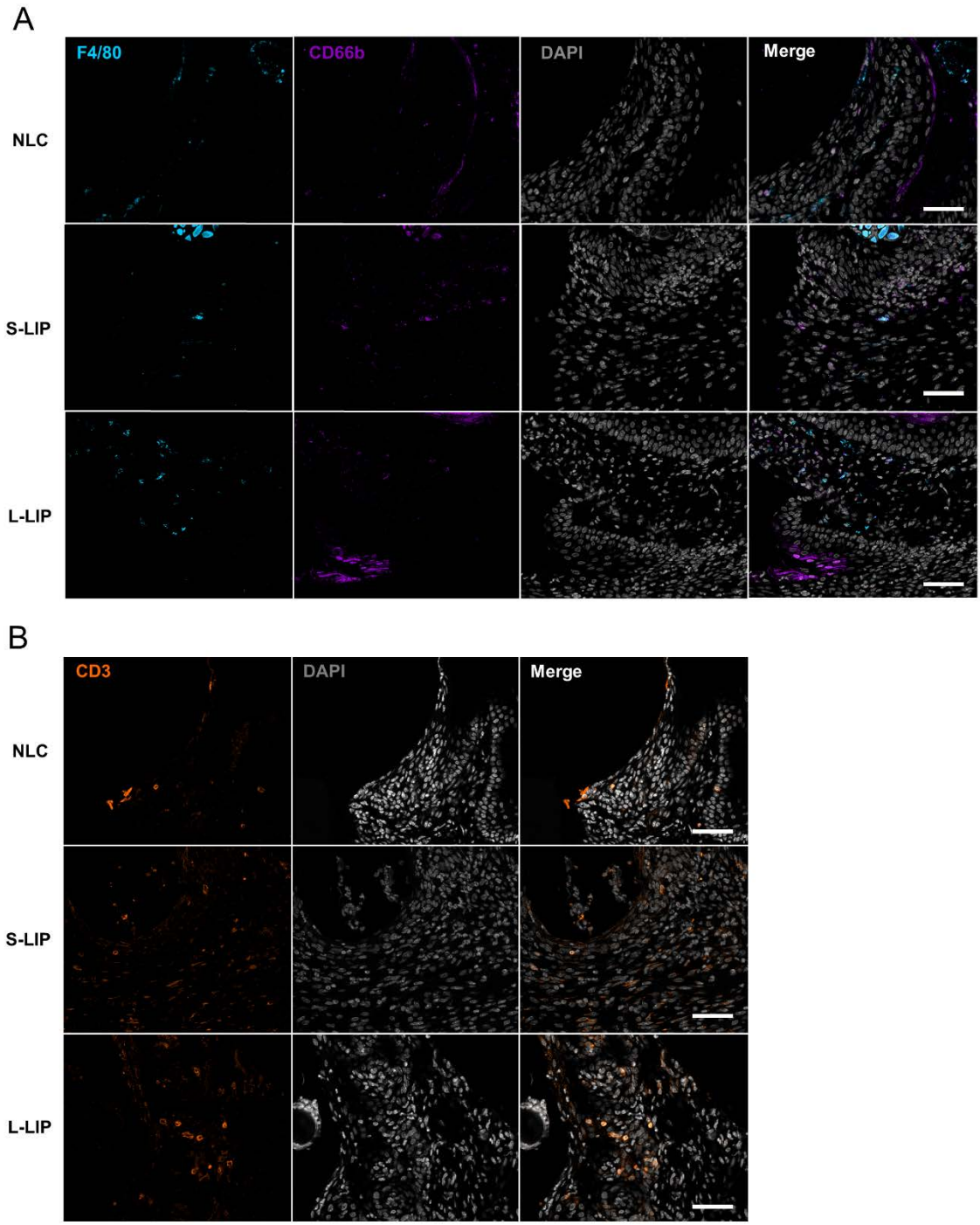

Appendix Figure 3.
A,B. Individual channels of the merged image in Figure 2D are shown. S-LIP, short-term ligature-induced periodontitis (3 weeks); L-LIP, long-term ligature-induced periodontitis (10 weeks), NLC, no-ligature control. Scale bar: 50μm.

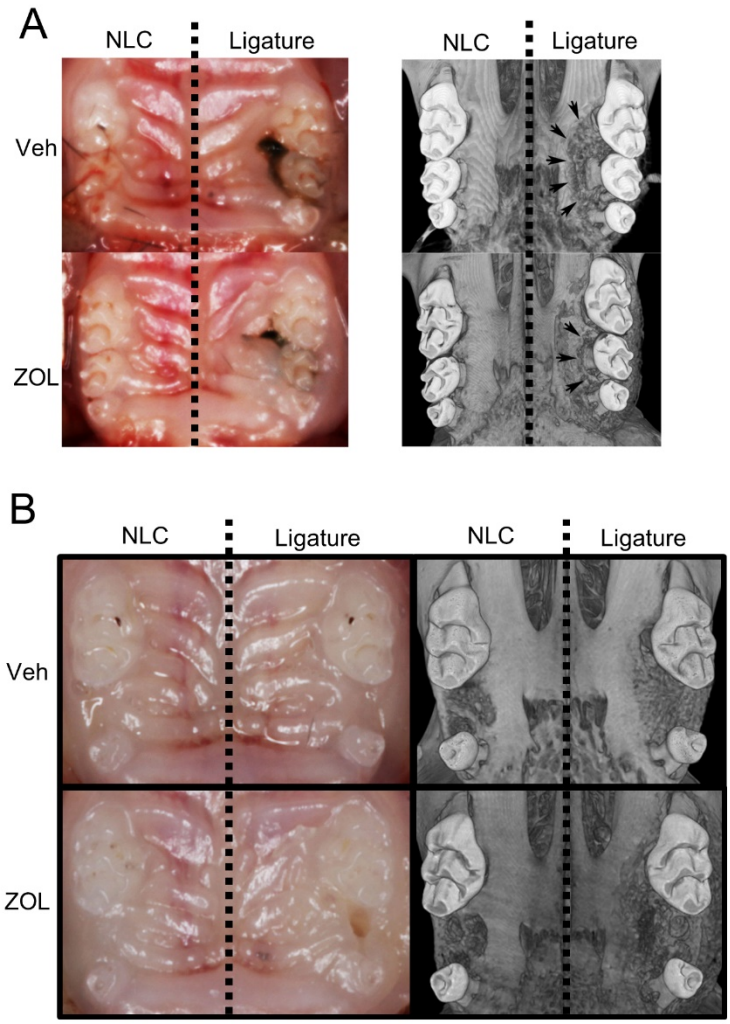

Appendix Figure 4.
A. Clinical (left) and µCT reconstructed photographs (right) depicting extent of tissue blanching caused by ligature placement and extent of palatal bone resorption (black arrowheads) in a model of L-LIP without tooth extraction. B. Clinical (left) and µCT reconstructed photographs (right) depicting oral mucosal healing and extent of palatal bone resorption (black arrowheads) in a model of L-LIP with tooth extraction.

A

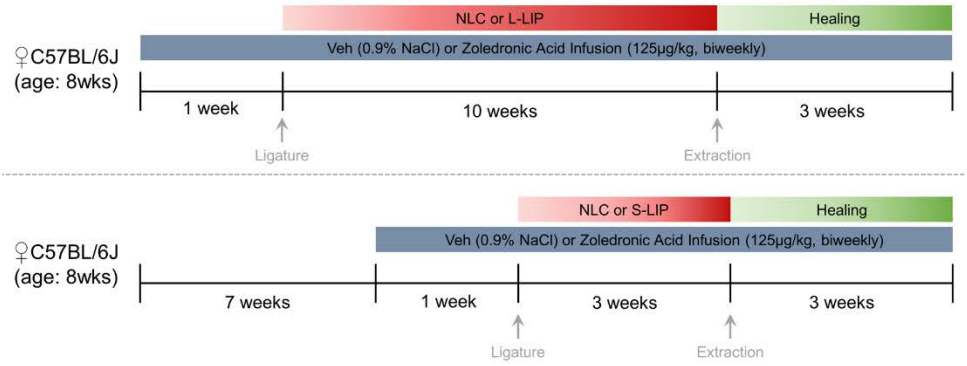
NLC or L-LIP
Healing
Veh (0.9% NaCl) or Zoledronic Acid Infusion (125μg/kg, biweekly)
♀C57BL/6J
(age: 8wks)
1 week
10 weeks
3 weeks
Ligature
Extraction
NLC or S-LIP
Healing
Veh (0.9% NaCl) or Zoledronic Acid Infusion (125μg/kg, biweekly)
♀C57BL/6J
(age: 8wks)
7 weeks
1 week
3 weeks
3 weeks
Ligature
Extraction

B

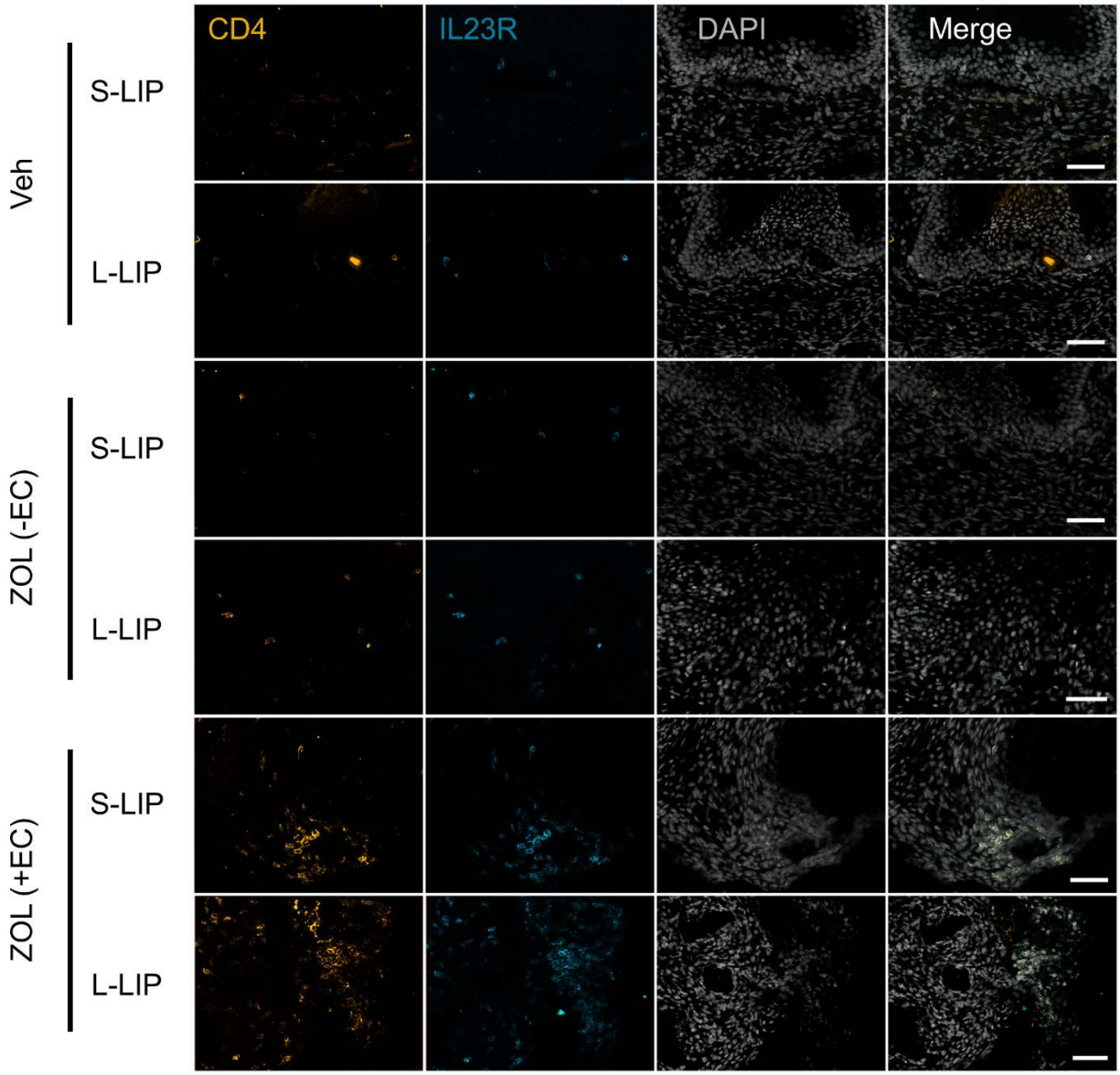
CD4
IL23R
DAPI
Merge
Veh
S-LIP
L-LIP
ZOL (-EC)
S-LIP
L-LIP
ZOL (+EC)
S-LIP
L-LIP

Appendix Figure 5.
A. In Figure 5, the mouse model in Figure 4A was directly compared to our previously published mouse model, where we induce periodontitis by ligature for 3 weeks in zoledronic acid treated mice, extract the ligated tooth and allow for 3 weeks of healing. B. Individual channels of the merged image in Figure 5E are shown. S-LIP, short-term ligature-induced periodontitis (3 weeks); L-LIP, long-term ligature-induced periodontitis (10 weeks); ZOL, zoledronic acid; EC, epithelial closure. Scale bar: 50μm.

References

Aghaloo T, Hazboun R, Tetradis S (2015). Pathophysiology of osteonecrosis of the jaws. *Oral Maxillofac Surg Clin North Am* 27:489–496.

Aghaloo TL, Kang B, Sung EC, Shoff M, Ronconi M, Gotcher JE, et al. (2011). Periodontal disease and bisphosphonates induce osteonecrosis of the jaws in the rat. *J. Bone Miner. Res.* 26:1871–1882.

Al-Rasheed A (2012). Elevation of white blood cells and platelet counts in patients having chronic periodontitis. *Saudi Dent. J.* 24:17–21.

Bain JL, Lester SR, Henry WD, Bishop CM, Turnage AA, Naftel JP, et al. (2009). Comparative gender differences in local and systemic concentrations of pro-inflammatory cytokines in rats with experimental periodontitis. *J. Periodontal Res.* 44:133–140.

Brousseau-Nault M, Kizhakkedathu JN, Kim H (2017). Chronic periodontitis is associated with platelet factor 4 (PF4) secretion: A pilot study. *J. Clin. Periodontol.* 44:1101–1111.

Caporaso JG, Kuczynski J, Stombaugh J, Bittinger K, Bushman FD, Costello EK, et al. (2010). QIIME allows analysis of high-throughput community sequencing data. *Nat. Methods* 7:335–336.

Caporaso JG, Lauber CL, Walters WA, Berg-Lyons D, Huntley J, Fierer N, et al. (2012). Ultra-high-throughput microbial community analysis on the Illumina HiSeq and MiSeq platforms. *ISME J.* 6:1621–1624.

Compston JE, McClung MR, Leslie WD (2019). Osteoporosis. *Lancet* 393:364–376.

Dutzan N, Kajikawa T, Abusleme L, Greenwell-Wild T, Zuazo CE, Ikeuchi T, et al. (2018). A dysbiotic microbiome triggers TH17 cells to mediate oral mucosal immunopathology in mice and humans. *Sci. Transl. Med.* 10.

Dutzan N, Konkel JE, Greenwell-Wild T, Moutsopoulos NM (2016). Characterization of the human immune cell network at the gingival barrier. *Mucosal Immunol.* 9:1163–1172.

Graves DT, Kang J, Andriankaja O, Wada K, Rossa C (2012). Animal models to study host-bacteria interactions involved in periodontitis. *Front. Oral Biol.* 15:117–132.

Greinacher A, Holtfreter B, Krauel K, Gätke D, Weber C, Ittermann T, et al. (2011). Association of natural anti-platelet factor 4/heparin antibodies with periodontal disease. *Blood* 118:1395–1401.

Harrison P, Cramer EM (1993). Platelet alpha-granules. *Blood Rev* 7:52–62.

Kalyan S, Wang J, Quabius ES, Huck J, Wiltfang J, Baines JF, et al. (2015). Systemic immunity shapes the oral microbiome and susceptibility to bisphosphonate-associated osteonecrosis of the jaw. *J. Transl. Med.* 13:212.

Kennel KA, Drake MT (2009). Adverse effects of bisphosphonates: implications for osteoporosis management. *Mayo Clin. Proc.* 84:632–7; quiz 638.

Kikuiri T, Kim I, Yamaza T, Akiyama K, Zhang Q, Li Y, et al. (2010). Cell-based immunotherapy with mesenchymal stem cells cures bisphosphonate-related osteonecrosis of the jaw-like disease in mice. *J. Bone Miner. Res.* 25:1668–1679.

Kim RH, Lee RS, Williams D, Bae S, Woo J, Lieberman M, et al. (2011). Bisphosphonates induce senescence in normal human oral keratinocytes. *J. Dent. Res.* 90:810–816.

Kim T, Kim S, Song M, Lee C, Yagita H, Williams DW, et al. (2018). Removal of Pre-Existing Periodontal Inflammatory Condition before Tooth Extraction Ameliorates Medication-Related Osteonecrosis of the Jaw-Like Lesion in Mice. *Am. J. Pathol.* 188:2318–2327.

Lescaille G, Coudert AE, Baaroun V, Ostertag A, Charpentier E, Javelot M-J, et al. (2014). Clinical study evaluating the effect of bevacizumab on the severity of zoledronic acid-related osteonecrosis of the jaw in cancer patients. *Bone* 58:103–107.

Li CL, Lu WW, Seneviratne CJ, Leung WK, Zwahlen RA, Zheng LW (2016). Role of periodontal disease in bisphosphonate-related osteonecrosis of the jaws in ovariectomized rats. *Clin. Oral Implants Res.* 27:1–6.

Marx RE (2003). Pamidronate (Aredia) and zoledronate (Zometa) induced avascular necrosis of the jaws: a growing epidemic. *J. Oral Maxillofac. Surg.* 61:1115–1117.

Neville-Webbe HL, Coleman RE (2010). Bisphosphonates and RANK ligand inhibitors for the treatment and prevention of metastatic bone disease. *Eur. J. Cancer* 46:1211–1222.

Nicu EA, Van der Velden U, Nieuwland R, Everts V, Loos BG (2009). Elevated platelet and leukocyte response to oral bacteria in periodontitis. *J. Thromb. Haemost.* 7:162–170.

Papapanagiotou D, Nicu EA, Bizzarro S, Gerdes VEA, Meijers JC, Nieuwland R, et al. (2009). Periodontitis is associated with platelet activation. *Atherosclerosis* 202:605–611.

Roelofs AJ, Thompson K, Gordon S, Rogers MJ (2006). Molecular mechanisms of action of bisphosphonates: current status. *Clin. Cancer Res.* 12:6222s–6230s.

Saadi-Thiers K, Huck O, Simonis P, Tilly P, Fabre J-E, Tenenbaum H, et al. (2013). Periodontal and systemic responses in various mice models of experimental periodontitis: respective roles of inflammation duration and Porphyromonas gingivalis infection. *J. Periodontol.* 84:396–406.

Song M, Alshaikh A, Kim T, Kim S, Dang M, Mehrazarin S, et al. (2016). Preexisting Periapical Inflammatory Condition Exacerbates Tooth Extraction-induced Bisphosphonate-related Osteonecrosis of the Jaw Lesions in Mice. *J Endod* 42:1641–1646.

Soundia A, Hadaya D, Esfandi N, Gkouveris I, Christensen R, Dry SM, et al. (2018). Zoledronate Impairs Socket Healing after Extraction of Teeth with Experimental Periodontitis. *J. Dent. Res.* 97:312–320.

Van den Steen PE, Proost P, Wuyts A, Van Damme J, Opdenakker G (2000). Neutrophil gelatinase B potentiates interleukin-8 tenfold by aminoterminal processing, whereas it degrades CTAP-III, PF-4, and GRO-alpha and leaves RANTES and MCP-2 intact. *Blood* 96:2673–2681.

Teronen O, Heikkilä P, Konttinen YT, Laitinen M, Salo T, Hanemaaijer R, et al. (1999). MMP inhibition and downregulation by bisphosphonates. *Ann. N. Y. Acad. Sci.* 878:453–465.

Thumbigere-Math V, Michalowicz BS, Hodges JS, Tsai ML, Swenson KK, Rockwell L, et al. (2014). Periodontal disease as a risk factor for bisphosphonate-related osteonecrosis of the jaw. *J. Periodontol.* 85:226–233.

Tong M, Jacobs JP, McHardy IH, Braun J (2014). Sampling of intestinal microbiota and targeted amplification of bacterial 16S rRNA genes for microbial ecologic analysis. *Curr. Protoc. Immunol.* 107:7.41.1–11.

Williams DW, Lee C, Kim T, Yagita H, Wu H, Park S, et al. (2014). Impaired bone resorption and woven bone formation are associated with development of osteonecrosis of the jaw-like lesions by bisphosphonate and anti-receptor activator of NF-κB ligand antibody in mice. *Am. J. Pathol.* 184:3084–3093.

Zhang Q, Atsuta I, Liu S, Chen C, Shi Shihong, Shi Songtao, et al. (2013). IL-17-mediated M1/M2 macrophage alteration contributes to pathogenesis of bisphosphonate-related osteonecrosis of the jaws. *Clin. Cancer Res.* 19:3176–3188.

Chapter 3

Commensal microbiota protects against inflammation-induced osteonecrosis following zoledronic acid infusion*

***In preparation for publication**

Abstract

Medication-related osteonecrosis of the jaw (MRONJ) is a rare intraoral lesion that occurs in patients with long-term and/or high-dose use of nitrogen-containing bisphosphonates such as zoledronic acid (ZOL). Previously, several studies have found increased microbial signatures present on human MRONJ lesion biopsies, but the role of the commensal microbiota in MRONJ pathogenesis is unknown. Here, we examined the role of the commensal microbiota in MRONJ development following extraction of healthy teeth and teeth with ligature-induced periodontitis (LIP). In support of previous findings, we show increased bacterial infiltration in MRONJ lesions compared to normal healed controls. We found that antibiotic-mediated oral dysbiosis leads to a local inhibition of bone resorption in the context of LIP. In our MRONJ model, antibiotic-treated animals (Abx) displayed distended ceca, involuted spleens, and significantly reduced oral and fecal bacterial loads compared to the specific-pathogen free (SPF) cohort. We observed no significant difference in empty lacunae, necrotic bone formation, osteoclast number and surface area in Abx and SPF animals following extraction of healthy teeth. However, extraction of LIP-teeth led to increased empty lacunae, necrotic bone, and osteoclast surface area in Abx compared to SPF mice. Our findings suggest that the commensal microbiome protects against LIP-induced osteonecrosis.

Introduction

Antiresorptive therapies (ART) including nitrogen-containing bisphosphonates like Zoledronic Acid (ZOL) are the first-line treatment of choice for osteoporosis treatment and critical in the prevention of skeletal metastases in cancer patients(Chen and Sambrook, 2011). Medication-related osteonecrosis of the jaw (MRONJ) is a rare but serious oral complication that typically occurs following dental interventions in patients taking ART for prolonged periods of time or at high doses(Marx et al., 2007). MRONJ is clinically defined as exposed bone that has persisted for over 8 weeks in patients who have no history of radiation exposure to the head and neck area(Ruggiero et al., 2014) but have been exposed to ART.

The barrier mucosal organs contain a robust epithelium that uniquely separates two contending cell populations: a diverse community of microorganisms that exert pleiotropic effects on host function(Shreiner et al., 2015); and a mixture of host immune, endothelial, and mesenchymal cells that form intricate networks for nutrient and antigen exchange (Chang et al., 2014). The coevolution of host and microbiota has resulted in a delicate and mutually beneficial system whereby the host provides microbes a niche with abundant carbon sources, and the microbes aid in digestion of complex carbohydrates (Flint et al., 2012). Unlike other barrier mucosal tissues, the oral cavity contains trans-mucosal organs (teeth) that lack tight junctions at their interface with the oral mucosa, making this area particularly susceptible to bacterial infiltration (Bosshardt and Lang, 2005). When commensal bacteria accumulate at sites directly adjacent to this interface they can become pathobionts that cause local inflammation leading to a host-mediated destruction of alveolar bone, clinically known as periodontitis (Darveau, 2010).

In early reports of MRONJ, 84% of patients had periodontal disease as a dental comorbidity and in 78% of the cases, the precipitating event that led to ONJ development was an extraction or dental surgery (Marx et al., 2005) which has been corroborated *in vivo* (Kim et al., 2018; Soundia et al., 2018; Aghaloo et al., 2011). Because periodontal disease is driven by local

microbial dysbiosis and extraction sites are in intimate contact with oral bacteria during healing, several groups have investigated the association between the oral microbiome and MRONJ lesion development. Scanning electron microscope analysis from MRONJ lesions has revealed microbial biofilm formation on sequestered bone (Sedghizadeh et al., 2008). Metagenomic analyses have been varied with respect to bacterial diversity in MRONJ patients (Pushalkar et al., 2014; Kalyan et al., 2015) but increased *Actinomyces spp.* accumulation on MRONJ lesions is a common finding (Marx et al., 2005; Kos et al., 2010). Moreover, a critical role for bacterial infections in MRONJ pathogenesis has been elucidated by studies showing a decrease in ONJ incidence in cancer patients who improved their oral hygiene (Ripamonti et al., 2009).

Existing literature overwhelmingly supports that ART, dental surgery, and local inflammatory disease are all risk factors for MRONJ development, however, the role of the microbiota in this pathologic condition is controversial. In this study, we investigate the role of the commensal microbiota in MRONJ pathogenesis by significantly reducing the oral and gastrointestinal microbiota with broad spectrum antibiotics followed by extraction of healthy or periodontally diseased teeth in vehicle (Veh) or ZOL treated mice.

Materials and Methods

Animals

6-week-old female C57BL/6J mice were purchased from the Jackson Laboratories and housed in a specific pathogen free (SPF) environment with 12-hour light/dark cycle managed by the UCLA Division of Laboratory and Animal Medicine. All experimental protocols were approved by institutional guidelines from the Chancellor's Animal Research Committee (2011-062).

Commensal microbiota reduction and ligature-induced periodontitis

SPF mice were randomly assigned into four groups: SPF+no ligature control (NLC), SPF+LIP, antibiotic-treated (Abx)+NLC and Abx+LIP groups (n=8 mice each). All Abx animals received twice daily intragastric and intraoral gavage of vancomycin (50mg/kg), metronidazole (100mg/kg) and neomycin (100mg/kg), with ampicillin (0.5mg/mL) provided in the drinking water *ad libitum* for the first 7 days of the study. Sterile saline gavage and unaltered water were delivered to SPF mice. After 7 days, a 6-0 silk suture was aseptically placed on the right and left second maxillary molar (M2) of Abx/LIP and SPF/LIP groups. For Abx animals, we maintained dysbiosis by delivering vancomycin (0.5mg/mL), ampicillin (1mg/mL) and neomycin (1mg/mL) in drinking water *ad libitum* for the remainder of the study. Three weeks after ligature placement, animals were sacrificed. A schematic illustrating the timeline of the study can be found in **Figure 3A**.

Commensal microbiota reduction and MRONJ

SPF mice were randomly assigned into six groups: SPF/Veh/NLC, SPF/ZOL/NLC, SPF/ZOL/LIP, Abx/Veh/NLC, Abx/ZOL/NLC, and Abx/ZOL/LIP (n=8-10 mice each). Animals in the SPF and Abx groups received unaltered water or antibiotic gavage/water as described above for the entire study. Animals receiving Veh and ZOL treatment received biweekly intravenous injections of 0.9% NaCl or 125μg/kg Zoledronic acid (Sagent Pharmaceuticals) starting one week after the study began and continuing throughout the study. Two weeks after the study began, animals in the LIP groups received a ligature as described above. 3 after

ligature placement, all animals underwent maxillary M2 extraction. Prior to sacrifice, oral and fecal samples were aseptically obtained and weighed. Following sacrifice, spleens and ceca were dissected and weights were compared to total body weight. A schematic illustrating the timeline of the study can be found in **Figure 4A**.

Micro-computed tomography

Whole maxillae were scanned with a voxel size of 10μm^3 using a 1.0 mm aluminum filter at 60 kVp and 166μA (SkyScan 1275; Bruker). Other scanning parameters include rotation step of 0.4 degrees, frame averaging of 6 and random movement. 2-dimensional images were reconstructed using N Recon (Bruker) following X-Y alignment and dynamic range adjustment. Reconstructed images were saved as 16-bit TIFF images and used for bone loss analysis. Bone loss was quantified by measuring the distance between cementoenamel junction and the alveolar ridge on the palatal, mesiobuccal and distobuccal roots of M2 using CTAn (Bruker). Net bone loss was assessed by subtracting SPF/NLC from SPF/LIP and Abx/NLC from Abx/LIP. 3-dimensional representative images were generated in CTVox (Bruker).

Histomorphometric and histochemical staining

Hematoxylin and eosin and tartrate-resistant acid phosphatase (#387A-1KT, Millipore Sigma) staining was performed following decalcification and paraffin embedding as described previously (Williams et al., 2014). Quantifications were performed using ImageJ and Histomorph(van 't Hof et al., 2017).

Quantitative real-time PCR

Bacterial DNA was extracted from fecal and oral samples of one animal per cage in both SPF and Abx groups taken before sacrifice using the DNeasy PowerSoil Kit (Qiagen; #12888-100). Real-time PCR of genomic DNA was performed to determine relative 16S rRNA expression in SPF and Abx groups using the universal primers (515F 5'-GTGCCAGCMGCCGCGGTAA-3'; 806R 5'-GGACTACHVGGGTWTCTAAT-3') with PowerUp SYBR Green Master Mix

(#100029284; Applied Biosystems) in a QuantStudio 3 Real-Time PCR System (Applied Biosystems).

16S rRNA sequencing

Bacterial DNA was extracted from fecal, oral, spleen and liver samples as described above. Library preparation was performed as described (Tong et al., 2014) using uniquely barcoded primers targeting the V4 region of the 16S gene (Caporaso et al., 2012). Pooled libraries diluted to 6pM in 20% PhiX underwent paired-end (2x250bp) sequencing using the Illumina MiSeq v2 platform. Demultiplexed sequencing results were analyzed with the QIIME pipeline (Caporaso et al., 2010).

Fluorescent *in situ* hybridization

Archived MRONJ samples (Williams et al., 2014) were deparaffinized in a 60°C oven and rehydrated in serial dilutions of xylene and ethanol. A custom probe targeting position 338-355 of the 16S rRNA bacterial gene was generated with a Cyanine-3 fluorescent tag for *in situ* hybridization (5'-[Cy3] GCT GCC TCC CGT AGG AGT- 3'; MilliporeSigma). The probe was diluted to 1μM in hybridization buffer (0.9M NaCl, 0.1% SDS, 20mM Tris-HCl) and slides were incubated for 4 hours at 50°C in a humidified chamber to allow for hybridization. Tissues were counterstained with 300nM DAPI for 5 minutes, mounted with Prolong Gold (Thermofisher), imaged on a Leica DMI8 epifluorescence microscope and quantified in the provided LAS software.

Statistical analysis

All data are shown as mean ± SEM. For all figures, differences between groups were compared by one- or two-way ANOVA with Tukey's post-hoc test, as appropriate. *$p < 0.05$; **$p < 0.01$; ***$p < 0.001$; ****$p < 0.0001$; ns, not statistically significant.

Results

MRONJ lesions are associated with increased bacterial infiltrate and antimicrobial gene expression

We previously identified a critical role for IL36 family cytokines in ONJ pathogenesis, whereby IL36 signaling disrupts osteomucosal healing by inhibiting collagen synthesis in primary mouse gingival mesenchymal stem cells (GMSCs) (Kim et al., 2017). To further understand how IL36 influences GMSC physiology, we exposed GMSCs to IL36α and performed microarray analysis to identify differentially expressed genes (DEG) (**Appendix Fig. 1A**). Identified DEGs clustered within biological pathways related to inflammation and infection, including IL17A signaling in fibroblasts, acute phase response signaling and IL6 signaling (**Appendix Fig. 1B**). Interestingly, of the top 10 most upregulated DEGs, 80% (8/10) are known to have direct or indirect antimicrobial function (**Appendix Fig. 1C**) and mapped to a single, highly connected protein network of physical and functional associations with IL6, a major effector of immunocompetence (**Appendix Fig. 1D**). The host response to MRONJ-associated cues combined with literature that shows IL36 cytokines are released in response to microbial stimulation (Jensen, 2017) supports the hypothesis that host defense against microbes may be an important factor in MRONJ pathogenesis.

MRONJ lesions are barrier defects that involve bone exposure in the maxillofacial region which inevitably becomes colonized by the oral microbiota. To determine the extent of microbial infiltration in murine MRONJ lesions, we assayed tissues generated from a previous study (**Fig 1A**, Williams et al., 2014). Utilizing FISH with a universal bacterial probe, we found significantly increased bacterial signatures in the connective tissue and epithelium of MRONJ lesions with exposed bone and unhealed epithelium compared to vehicle treated controls that had complete epithelial closure and no exposed bone (**Fig. 1B**). This data identifies a bacterial component that is unique to MRONJ lesions.

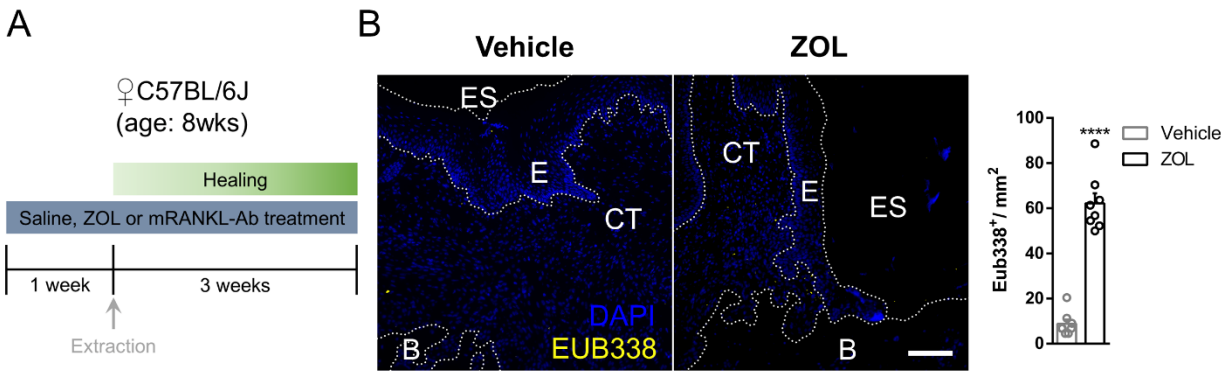

Figure 1. Increased microbial infiltrate in MRONJ lesions.
A. Experimental schematic of the previously published study. B. Fluorescence *in situ* hybridization of 16S rRNA using the universal bacterial probe Eub338 conjugated to Cy3. ES, extraction site; E, epithelium; CT, connective tissue; B, bone; Veh, vehicle; ZOL, zoledronic acid. **** $p<0.0001$. Scale bar: 100µm

Broad spectrum antibiotic treatment modifies host physiology and microbiota composition

To understand the role of the microbiota in MRONJ pathogenesis, we utilized a model of systemic dysbiosis achieved by drastically reducing the commensal microbiota (Reikvam et al., 2011). Mice treated with antibiotics (Abx) for at least four weeks showed more than 99% decrease in the bacteria-specific 16S rDNA gene expression compared to specific pathogen free (SPF) controls from equal amounts of fecal or oral swab material (**Fig. 2A**). Spleen size as a percentage of body weight was almost halved in Abx mice compared to SPF mice (**Fig. 2B**). Conversely, Abx mice developed enlarged ceca that weighed an average of four times more than ceca from SPF controls (**Fig. 2C**). 16S rDNA sequencing of oral swabs revealed significantly more alpha diversity in Abx compared to SPF groups (**Fig. 2D**), while Bray-Curtis principal coordinate analysis and taxonomic bar plots showed that SPF and Abx samples were comprised of significantly different bacterial taxa (**Fig. 2E,F**). Together, this data demonstrates a robust experimental system to study the role of the oral commensal microbiome in the development of oral disease.

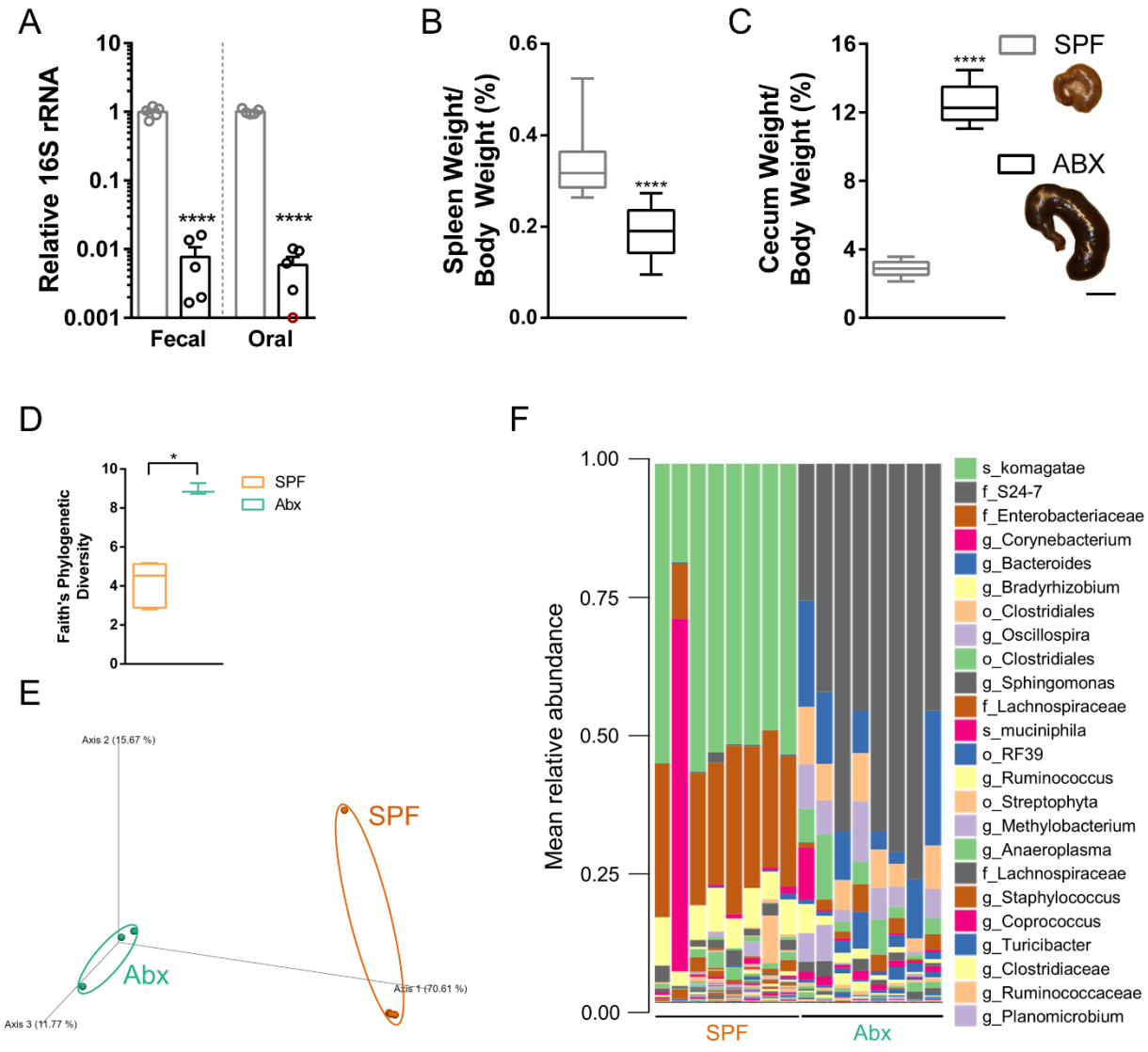

Figure 2. Broad spectrum antibiotic treatment leads to macroscopic germ-free phenotype in mice.

Figure 2. Broad spectrum antibiotic treatment leads to macroscopic germ-free phenotype in mice. A. 16S rRNA quantitative real-time PCR was performed from genomic DNA extracted from fecal and oral samples collected prior to sacrifice. One oral sample fell below the C_t cutoff of 40 and was placed on the X-axis in red. B, C. Spleen (B) and cecum (C) weights are presented as a percentage of total animal body weight at the time of sacrifice. Representative images of ceca from SPF and Abx groups on the far right. D,E. The alpha (D) and beta (E) diversity of the microbial communities found at the site of ligature placement were calculated by Faith's phylogenetic diversity and Bray-Curtis dissimilarity principal component analysis, respectively. F. Microbiome composition is shown at the amplicon sequence variant level (ASV). The top 24 ASVs are classified at the highest taxonomic level identified by sequencing. s_, species; g_, genus; f_, family. **** $p < 0.0001$. Scale bar: 10mm.

Antibiotic-induced dysbiosis alters maxillary bone homeostasis in health and disease

To determine how the commensal microbiota influences maxillary bone homeostasis in the absence of confounding variables such as ART or tooth extraction, we compared alveolar bone height and maxillary bone mass following LIP in SPF and Abx mice (**Fig. 3A**). µCT imaging and cemento-enamel junction (CEJ) to alveolar bone crest (ABC) distance reveal that LIP induces significant alveolar bone loss in both SPF and Abx mice compared to no-ligature controls (NLC), and there is a significant increase in CEJ-ABC distance in SPF compared to Abx animals with LIP (**Fig. 3B,C**). By the end of the 4 week study there was also a significant increase in CEJ-ABC distance on buccal roots of SPF/NLC compared to Abx/NLC animals (**Fig. 3B,C**).

Gut microbiota perturbation has been shown to regulate long-bone and vertebral bone mass in both germ-free and Abx mice (**Appendix Fig. 3,** Sjögren et al., 2012; Yan et al., 2016). However, it is unknown whether disruption of the commensal microbiota alters maxillary bone mass in a similar manner. In our model, bone loss on buccal but not palatal roots was significantly different between SPF and Abx animals (**Fig. 3C**). We therefore compared bone mass surrounding the buccal roots of each of our four animal cohorts. In contrast to long bone, maxillary bone mass and trabecular structure is not significantly altered by systemic dysbiosis. Although the relative CEJ-ABC distance was significantly increased, LIP does not alter buccal bone mass and trabecular structure in Abx animals whereas buccal bone mass is significantly decreased in SPF/LIP animals (**Fig. 3D-H**). This is evident qualitatively by observing porous buccal bone in SPF/LIP animals and smooth buccal bone in Abx/LIP animals (**Fig. 3B**). This suggests that the oral commensal microbiota plays an important role in maxillary bone mass regulation in both health and disease.

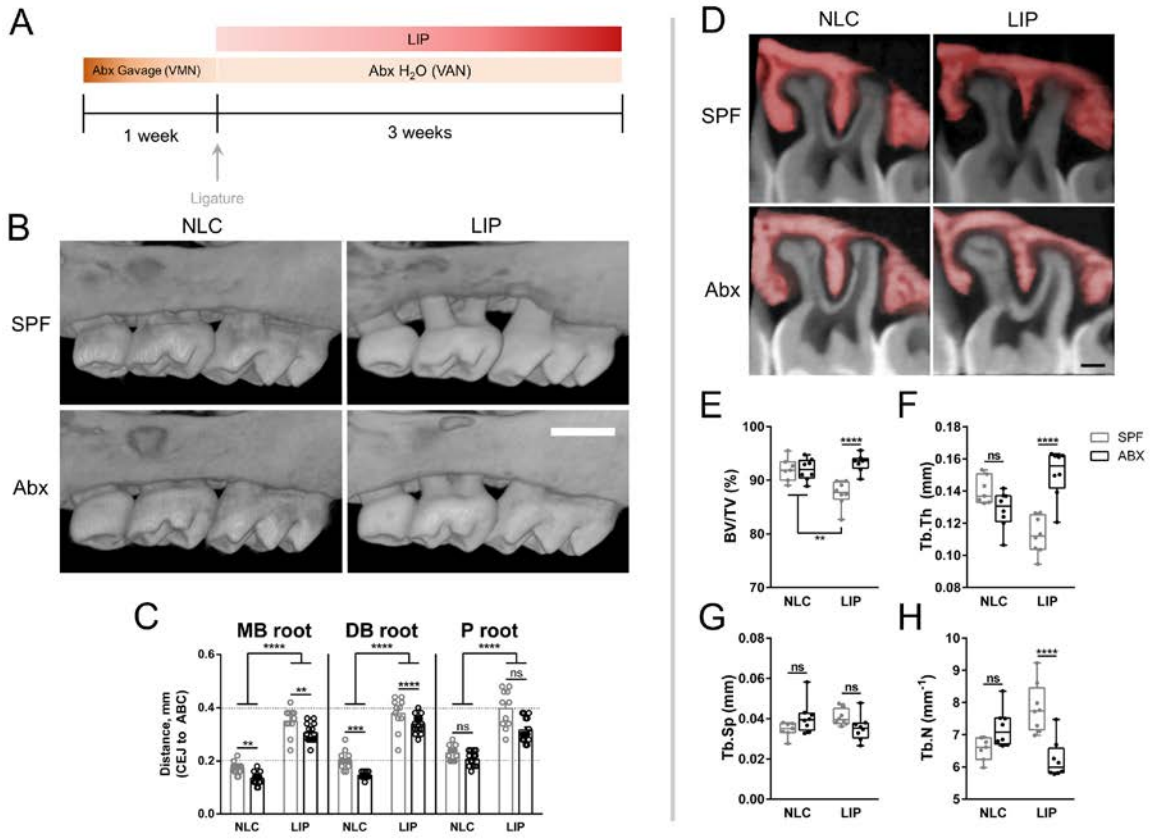

Figure 3. Systemic dysbiosis prevents alveolar bone loss and bone mass reduction following LIP
A. Schematic of mouse model. Antibiotics were administered by intragastric gavage for the first week and *ad libitum* in drinking water for subsequent weeks. One week after initial antibiotic administration, a 6-0 silk ligature was placed around the second maxillary molar. B. Representative buccal views of µCT reconstructed maxillae from SPF (top) or Abx (bottom) animals with (right) or without (left) ligature-induced periodontitis. Scale bar (white): 500µm. C. Quantification total distance from the cemento-enamel junction (CEJ) to the alveolar bone crest (ABC) measured from each of 3 roots on the second maxillary molar. D. Graphical representation of bone included in bone mass quantification at the buccal roots of the second maxillary molar. Bone included in analysis has been pseudocolored in red for easy visualization. Scale bar (black): 200µm. E-H. 3-dimensional bone morphometric properties of buccal bone in (D) including bone mass (E), trabecular thickness (F), trabecular separation (G) and trabecular number (H). SPF, specific pathogen free; Abx, antibiotic-treated; NLC, non-ligature control; LIP, ligature-induced periodontitis; MB, mesio-buccal; DB, disto-buccal; P, palatal; BV/TV, bone volume per tissue volume; Tb.Th, trabecular thickness; Tb.Sp, trabecular separation; Tb.N, trabecular number. ns p>0.05; * p<0.05; ** p<0.01; *** p<0.001; **** p<0.0001.

Commensal microbiota protects against inflammation induced osteonecrosis

A histologic hallmark of ZOL-induced osteonecrosis is an increase in empty lacunae which is associated with reduced bone remodeling (Bonewald, 2011). To determine the role of the commensal microbiota in the pathogenesis of ZOL-induced osteonecrosis, we examined the number of empty lacunae and amount of necrotic bone in SPF and Abx animals treated with ZOL and LIP (**Fig. 4A**). ZOL treatment led to a significant increase in empty lacunae and necrotic bone compared to Veh treated controls but antibiotic treatment had no influence on these metrics (**Fig. 4B-D**). As expected based on previous findings (Kim et al., 2018), ZOL-treated mice that had LIP prior to extraction developed significantly more osteonecrosis compared to ZOL treatment alone. However, perturbation of the commensal microbiota with antibiotics resulted in a further increase in osteonecrosis compared to SPF animals with normal microbiota (**Fig. 4B-D**). This data suggests that disruption of the microbiota with antibiotics combined with local inflammation preceding a tooth extraction increases the development of osteonecrosis during ZOL therapy.

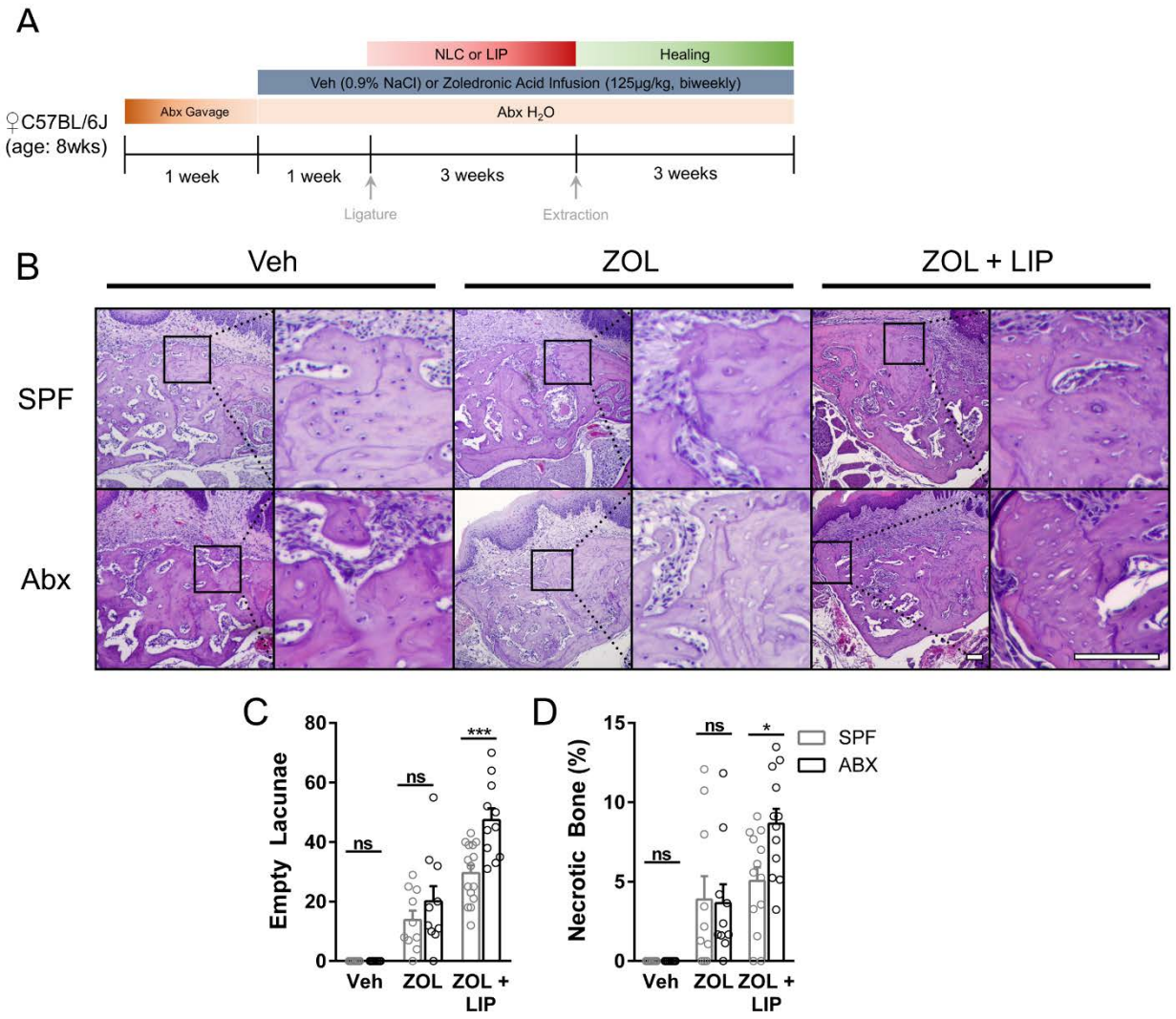

Figure 4: Histologic assessment of osteonecrosis formation in dysbiotic mice.
A. Hematoxylin and eosin section staining at the site of extraction. Representative images from each animal cohort are shown at two magnifications. Scale bar: 100um. B. The number of osteocyte lacunae without nuclear stain were quantified as empty lacunae. C. Areas containing more than 3 empty lacunae were quantified as necrotic and are presented as a percentage of the total bone present. All quantified data represent mean ± SEM. *p<0.05; ***p<0.001; ns, not statistically significant.

Antibiotic-induced dysbiosis increases osteoclast number and surface during inflammation induced osteonecrosis

We have previously shown that biweekly ZOL infusions increase TRAP positive osteoclasts 3 weeks after healthy or diseased tooth extraction occurs (Williams et al., 2014; Kim et al., 2018). To understand the role of microbial dysbiosis on resorptive cell numbers and surface area, we utilized enzyme histochemistry to identify TRAP positive osteoclasts at the site of extraction in Abx and SPF animals (**Fig. 5A**). ZOL infusions increased osteoclast number (**Fig. 5B**) and surface (**Fig. 5C**) in both Abx and SPF tissues following healthy tooth extraction. Interestingly, Abx tissues from LIP groups showed an increase in both osteoclast number and surface compared to SPF tissues (**Fig. 5B,C**). This data suggests that in the setting of bisphosphonate treatment and periodontal inflammation, the commensal microbiota dampens the generation of osteoclasts (**Fig. 6**).

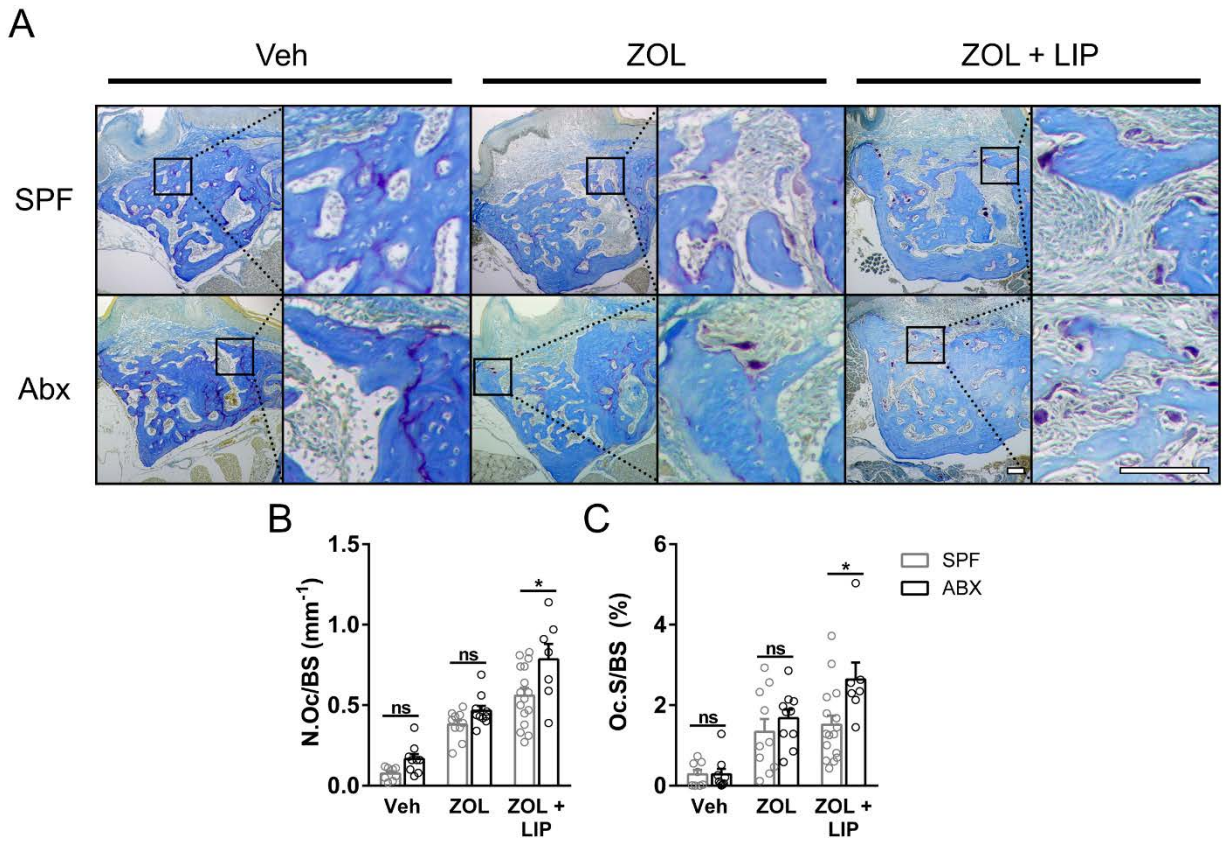

Figure 5: Histologic assessment of TRAP-positive osteoclasts in dysbiotic mice.
A. TRAP staining (purple) with aniline blue counterstain at the site of extraction. Representative images from each animal cohort are shown at two magnifications. Scale bar: 100μm. B,C. The number (B) and surface (C) of $TRAP^{+}$ osteoclasts per bone surface were quantified. Data is presented as mean ± SEM. *p<0.05; ns, not statistically significant.

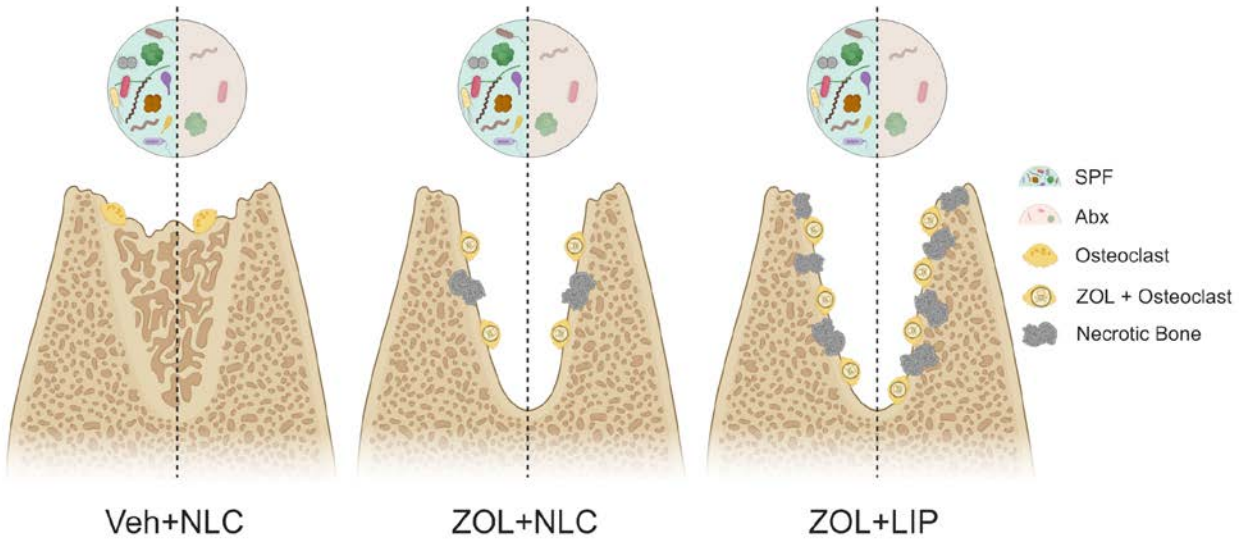

Figure 6: Proposed model.
Antibiotic perturbation of the oral microbiota does not alter the number of osteoclasts or necrotic bone formation following extraction of teeth in periodontal health (Left) or extraction of teeth in periodontal health with zoledronic acid (ZOL) treatment (Middle). Following extraction of a tooth with periodontal disease combined with ZOL therapy antibiotic-induced dysbiosis leads to increases in the amount of necrotic bone and number of osteoclasts at the extraction site (Right). Veh, vehicle; NLC, no-ligature control; ZOL, zoledronic acid; LIP, ligature-induced periodontitis.

Discussion

In this study, we provide *in vivo* evidence of increased bacterial infiltration in murine MRONJ-like lesions and show that local cells respond to MRONJ-associated inflammatory cues by upregulating antimicrobial genes *in vitro* (**Fig. 1, Appendix Fig. 1**). We also demonstrate host anatomical and microbiome changes associated with antibiotic-induced microbial reduction (**Fig. 2**). We identify the role of the commensal microbiota in LIP-induced bone loss (**Fig. 3**) and, for the first time, show a protective role for the commensal microbiota in inflammation-induced osteonecrosis development (**Fig. 4,5**). Cumulatively, our data reveals insight into how host-microbe interactions are important for bone physiology in the oral-maxillofacial region.

The keystone pathogen in periodontitis, *Porphyromonas gingivalis*, and the pathobionts that mediate subsequent inflammatory bone loss are members of the commensal microbiota and only become pathogenic under conditions where microbial homeostasis is not maintained (Hajishengallis, 2014). To delineate the role of the commensal microbiota in LIP-induced bone loss and subsequent osteonecrosis development, we developed a regimen of antibiotic treatment modified from Reikvam et al., aimed at significantly depleting the oral and gastrointestinal commensal microbiota. To reduce antibiotic resistance, our antibiotic cocktail has dual activity against gram positive (vancomycin and ampicillin) and negative (neomycin and ampicillin) aerobic bacteria, as well as activity against anaerobic bacteria (metronidazole). A potential confounding factor in this schema is non-specific effects from systemic antibiotic absorption that cause alterations in bone mass regulation, however BALB/c mice exposed to vancomycin (an antibiotic known to be poorly absorbed systemically) displayed the same high bone mass phenotype as mice who received a broad spectrum antibiotic cocktail similar to the one used in the current study (Yan et al., 2016).

In our study, Abx mice phenocopied physiologic characteristics of germ-free mice and displayed over 99% reduction in oral and gut microbes measured by 16S rDNA expression. The enlarged

cecum observed in germ-free and antibiotic-treated mice is a physiologic response to a reduction of indigenous gut bacteria. Dysbiosis leads to impaired water absorption in the colon but not the cecum causing the ceca of these animals to store an unusually high amount of water (Gordon and Pesti, 1971). The spleen is an immune organ that is important in producing and storing innate and adaptive immune cells. As the immune system is highly dependent on signals from both pathogenic and commensal microbiota, reduced microbiota stimulus in antibiotic treated animals leads to reduced spleen size (Kennedy et al., 2018). Taxonomic analysis and Bray-Curtis principal coordinate analysis revealed that in addition to a reduction of bacterial biomass (**Fig. 2A**), antibiotic perturbation changed the community composition of bacteria from that of mostly *Methylobacterium komagatae* and *Enterobacteriaceae* to *Bacteroidales* family *S24-7*, a family of uncultivatable bacteria primarily found in the gut of laboratory animals (Lagkouvardos et al., 2016, **Fig 2E,F**). These phenotypic characteristics combined with 16S rDNA expression and 16S sequencing confirms a significant reduction and alteration of indigenous oral microbiota in our study (**Fig. 2**).

In our approach, we target the oral and gut microbiota for both practical and clinical reasons. In order to completely digest their food and obtain essential nutrients broken down by gut microbes, rodents are coprophagic and expose the oral cavity to intestinal microbes during their daily routine (Soave and Brand, 1991). This inherent rodent activity would make it impossible to reduce the oral microbiota without also reducing the intestinal microbiota in standard solid-bottom cages. Additionally, our systemic dysbiosis model is clinically relevant because conservative treatment strategies include systemic antibiotic treatment in combination with oral antibacterial rinses for Stage 0 patients with no clinical signs of MRONJ (Ruggiero et al., 2014).

MRONJ pathogenesis is still incompletely understood, owing to its relatively recent discovery and multifactorial nature. A number of hypotheses to explain its etiology have been proposed that include bone remodeling inhibition, infection and inflammation, angiogenesis inhibition, soft

tissue toxicity, and innate or acquired immune dysfunction (Aghaloo et al., 2015). Through studies in our lab and others, it has become clear that bone remodeling inhibition is a central factor in the development of ONJ because current ARTs directly inhibit osteoclastic bone resorption (Aghaloo et al., 2011; Williams et al., 2014). Interestingly, the only other class of drugs known to cause MRONJ are anti-angiogenic agents such as vascular endothelial growth factor inhibitors and tyrosine kinase inhibitors (Nicolatou-Galitis et al., 2012). While these drugs are targeted monoclonal antibodies, as a class they have significant untargeted effects on bone metabolism (Alemán et al., 2014).

One effect of ART and anti-angiogenic therapy in rodents is a significant increase in long-bone trabecular bone mass (Williams et al., 2014). Significant osteopetrosis is also observed in germ-free and Abx adult mice (Sjögren et al., 2012; Yan et al., 2016). In Abx mice with biweekly ZOL infusions, distal femur trabecular bone mass plateaus at the same level observed in SPF/ZOL mice (**Appendix Fig. 3**). The increased bone mass in Abx/ZOL mice compared to Abx/Veh mice is not additive suggesting that Abx-mediated osteopetrosis is driven by a similar mechanism as ZOL-mediated osteopetrosis, which is an inhibition of osteoclast function. While in agreement with current theories derived from germ-free studies (Ohlsson and Sjögren, 2015), further investigation is required to confirm this hypothesis given the inherent immunophenotypic differences between germ-free and conventionally raised Abx mice.

In line with the bone remodeling inhibition hypothesis for MRONJ pathogenesis, we see no evidence of osteonecrosis in mice until they are treated with ZOL (**Fig. 4**). We also observe comparable levels of osteonecrosis in ZOL animals regardless of commensal microbiota perturbation, as these animals have similar bone mass and amounts of TRAP-positive osteoclasts (**Fig. 4, 5, Appendix Fig. 3**). In the absence of ART, dysbiotic animals with LIP maintain a significantly higher local bone mass compared to SPF/LIP animals (**Fig. 3D,E**). The consequence of increased systemic inhibition of osteoclasts by ZOL and local bone mass

maintenance in Abx/LIP results in significantly more osteonecrosis development in Abx/ZOL/LIP compared to SPF/ZOL/LIP animals, which coincides with an increased number of TRAP-positive osteoclasts (**Fig. 4, 5**). Therefore, this study provides further evidence that bone remodeling inhibition is a critical factor in MRONJ pathogenesis.

In line with the bone remodeling inhibition hypothesis for MRONJ pathogenesis, we see no evidence of osteonecrosis in mice until they are treated with ZOL (**Fig. 4**). We also observe comparable levels of osteonecrosis in ZOL animals regardless of commensal microbiota perturbation, as these animals have similar bone mass and amounts of TRAP-positive osteoclasts (**Fig. 4, 5, Appendix Fig. 3**). In the absence of ART, dysbiotic animals with LIP maintain a significantly higher local bone mass compared to SPF/LIP animals (**Fig. 3D,E**). The consequence of increased systemic inhibition of osteoclasts by ZOL and local bone mass maintenance in Abx/LIP results in significantly more osteonecrosis development in Abx/ZOL/LIP compared to SPF/ZOL/LIP animals, which coincides with an increased number of TRAP-positive osteoclasts (**Fig. 4, 5**). Therefore, this study provides further evidence that bone remodeling inhibition is a critical factor in MRONJ pathogenesis. In the context of our study, the increase in TRAP+ osteoclasts combined with an inhibition of bone resorption at the site of ligature placement suggests that the oral microbiota has a net catabolic effect on maxillary bone. Thus, the increase in necrotic bone seen in Abx/ZOL/LIP mice likely occurs due to a local inhibition of bone resorption brought on by the reduction of commensal microbiota.

Early studies reported that germ-free rats fail to develop significant inflammatory response and pathologic bone loss following placement of a ligature for up to 18 weeks (Rovin et al., 1966), yet recent work has shown that ligature placement in germ-free mice induces epithelial inflammation that is independent of bacterial colonization (Jiao et al., 2013). Additionally, it was reported that antibiotic treatment significantly reduces CEJ-ABC distance relative to non-antibiotic treated mice (Abe and Hajishengallis, 2013) which agrees with our observations (**Fig.**

3B,C). Together, these studies suggest that the ligature itself elicits a host response that likely arises from its direct communication with mouse gingival tissue. The constant barrage of mechanostimulatory signals from mastication is a unique feature of the oral barrier compared to the gut or skin and uniquely drives local immune cell development, including Th17 cells that are intimately involved in pathologic periodontal bone loss (Dutzan et al., 2017). Following significant reduction of oral microbiota contribution in LIP pathogenesis, we observed increased osteonecrosis development in Abx/ZOL/LIP mice, suggesting that trauma or damage is another integral factor in MRONJ pathogenesis. In fact, the specificity of MRONJ to the jaw region may be due in part to tissue-specific signals that occur in response to mechano-stimulation that cause barrier damage.

In summary, our study reveals that the commensal microbiota protects against osteonecrosis development in a mouse model of LIP but has no effect on osteonecrosis development in periodontal health. Broad spectrum antibiotic treatment is a recommended strategy in the management of MRONJ starting from Stage 0, and while our model represents an amount of antibiotic treatment that well exceeds recommendations, it suggests that targeted narrow spectrum therapy should be utilized to prevent deleterious disruptions to the commensal microbiota.

Appendix

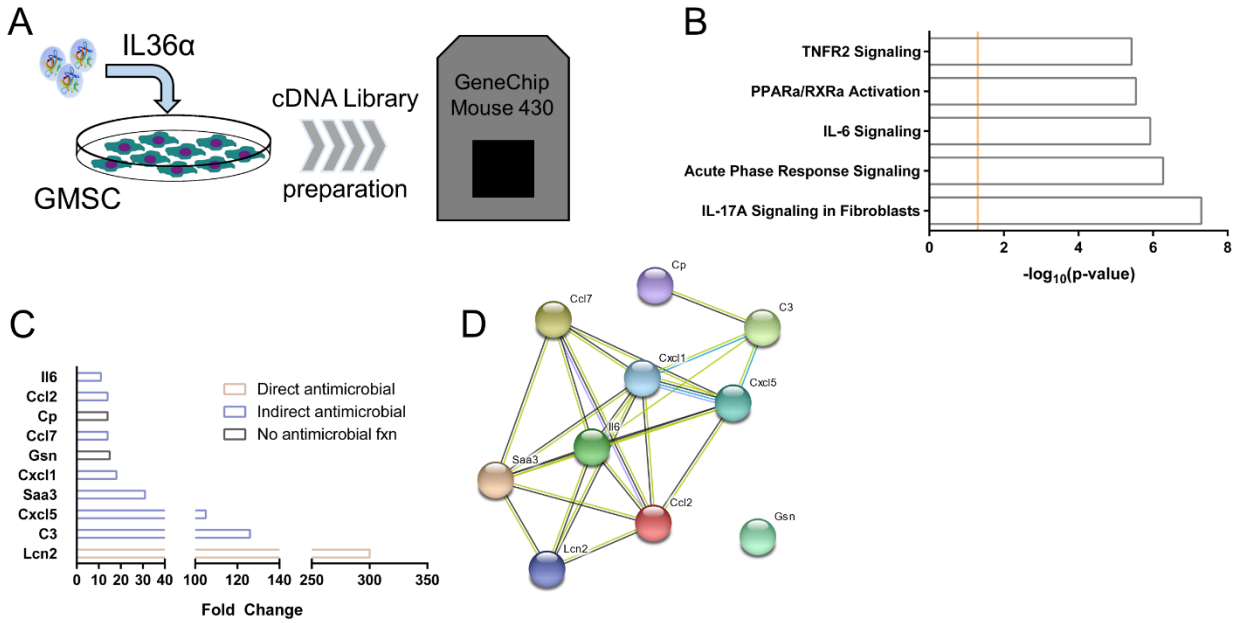

Appendix Figure 1.
A. Schematic of the *in vitro* workflow including cell culture, library preparation, and Affymetrix GeneChip Mouse Genome 430 2.0 microarray. B. Ingenuity pathway analysis showing the top 5 pathways upregulated in IL-36α treated GMSC. Yellow line at 1.3 denotes the boundary of statistical significance correlating to $p < 0.05$. C. Top 10 upregulated genes resulting from the microarray analysis color coded based on known direct or indirect antimicrobial properties. D. A node-based representation of the predicted and known protein-protein associations between upregulated genes in C. The colored lines represent the following: Yellow - predicted interaction from text mining; Purple - experimentally determined interaction; Black - co-expressed; Blue - interaction from curated database.

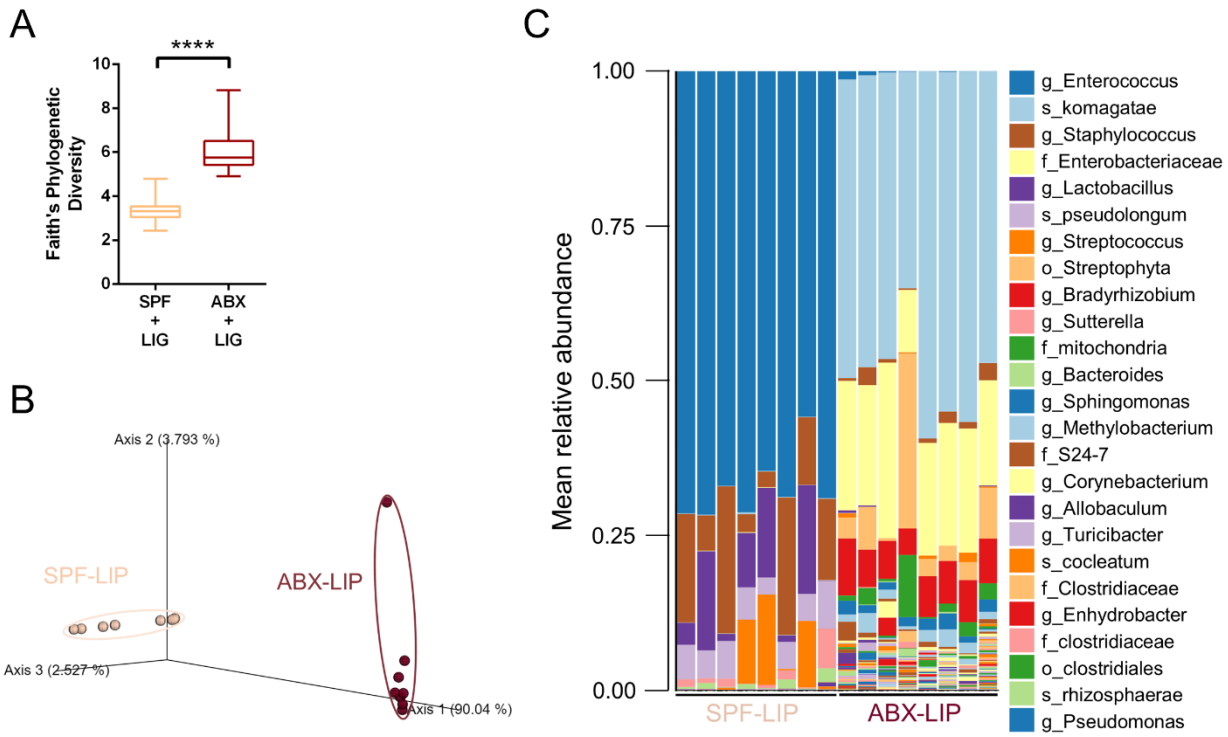

Appendix Figure 2.
A,B. The alpha (A) and beta (B) diversity of the microbial communities found at the site of ligature placement were calculated by Faith's phylogenetic diversity and Bray-Curtis dissimilarity principal component analysis, respectively. C. Microbiome composition is shown at the amplicon sequence variant level (ASV). The top 25 ASVs are classified at the highest taxonomic level identified. s_, species; g_, genus; f_, family. LIP, ligature-induced periodontitis. ****p<0.0001. Data is presented as a min/max box and whisker plot.

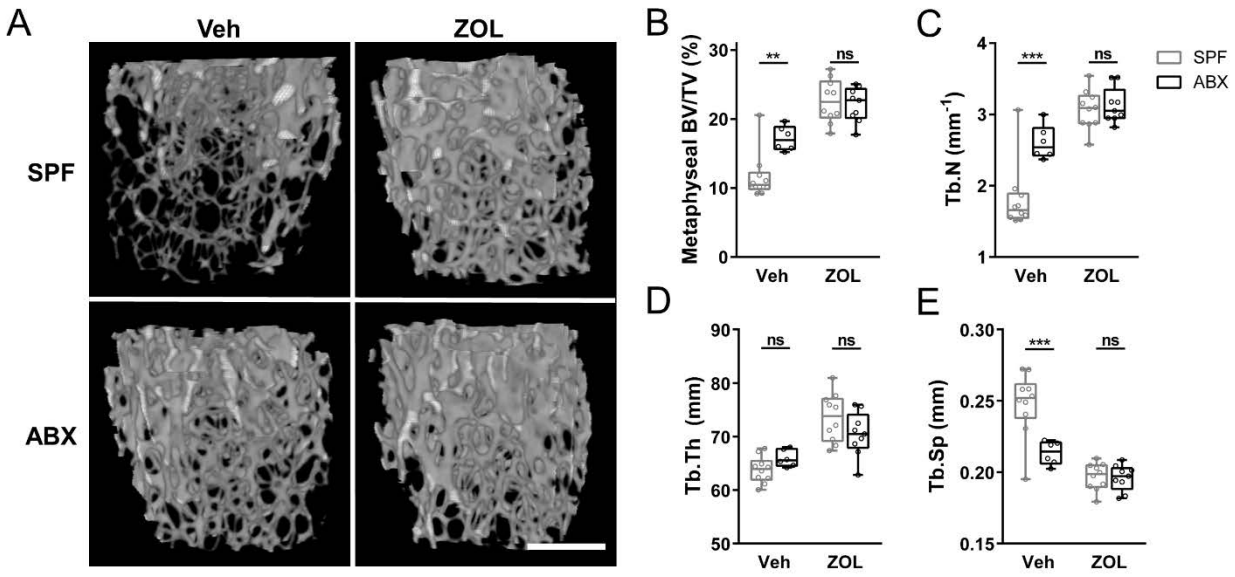

Appendix Figure 3.
A. Representative images of the metaphyseal trabecular bone from the distal femur. Scale bar: 500μm. B-E. Quantification of bone mass (B), trabecular number (C), trabecular thickness (D), and trabecular separation (E) measured from the region pictured in (A). SPF, specific pathogen free; Abx, antibiotic treated; Veh, vehicle; ZOL, zoledronic acid; BV/TV, bone mass percentage; Tb.N, trabecular number; Tb.Th, trabecular thickness; Tb.Sp, trabecular separation. **p<0.01; ***p<0.001.

References

Abe T, Hajishengallis G (2013). Optimization of the ligature-induced periodontitis model in mice. *J. Immunol. Methods* 394:49–54.

Aghaloo T, Hazboun R, Tetradis S (2015). Pathophysiology of osteonecrosis of the jaws. *Oral Maxillofac Surg Clin North Am* 27:489–496.

Aghaloo TL, Kang B, Sung EC, Shoff M, Ronconi M, Gotcher JE, et al. (2011). Periodontal disease and bisphosphonates induce osteonecrosis of the jaws in the rat. *J. Bone Miner. Res.* 26:1871–1882.

Alemán JO, Farooki A, Girotra M (2014). Effects of tyrosine kinase inhibition on bone metabolism: untargeted consequences of targeted therapies. *Endocr. Relat. Cancer* 21:R247–59.

Bonewald LF (2011). The amazing osteocyte. *J. Bone Miner. Res.* 26:229–238.

Bosshardt DD, Lang NP (2005). The junctional epithelium: from health to disease. *J. Dent. Res.* 84:9–20.

Caporaso JG, Kuczynski J, Stombaugh J, Bittinger K, Bushman FD, Costello EK, et al. (2010). QIIME allows analysis of high-throughput community sequencing data. *Nat. Methods* 7:335–336.

Caporaso JG, Lauber CL, Walters WA, Berg-Lyons D, Huntley J, Fierer N, et al. (2012). Ultra-high-throughput microbial community analysis on the Illumina HiSeq and MiSeq platforms. *ISME J.* 6:1621–1624.

Chang S-Y, Ko H-J, Kweon M-N (2014). Mucosal dendritic cells shape mucosal immunity. *Exp Mol Med* 46:e84.

Chen JS, Sambrook PN (2011). Antiresorptive therapies for osteoporosis: a clinical overview. *Nat. Rev. Endocrinol.* 8:81–91.

Darveau RP (2010). Periodontitis: a polymicrobial disruption of host homeostasis. *Nat. Rev. Microbiol.* 8:481–490.

Dutzan N, Abusleme L, Bridgeman H, Greenwell-Wild T, Zangerle-Murray T, Fife ME, et al. (2017). On-going Mechanical Damage from Mastication Drives Homeostatic Th17 Cell Responses at the Oral Barrier. *Immunity* 46:133–147.

Flint HJ, Scott KP, Duncan SH, Louis P, Forano E (2012). Microbial degradation of complex carbohydrates in the gut. *Gut Microbes* 3:289–306.

Gordon HA, Pesti L (1971). The gnotobiotic animal as a tool in the study of host microbial relationships. *Bacteriol Rev* 35:390–429.

Hajishengallis G (2014). Immunomicrobial pathogenesis of periodontitis: keystones, pathobionts, and host response. *Trends Immunol.* 35:3–11.

Jensen LE (2017). Interleukin-36 cytokines may overcome microbial immune evasion strategies that inhibit interleukin-1 family signaling. *Sci. Signal.* 10.

Jiao Y, Darzi Y, Tawaratsumida K, Marchesan JT, Hasegawa M, Moon H, et al. (2013). Induction of bone loss by pathobiont-mediated Nod1 signaling in the oral cavity. *Cell Host Microbe* 13:595–601.

Kalyan S, Wang J, Quabius ES, Huck J, Wiltfang J, Baines JF, et al. (2015). Systemic immunity shapes the oral microbiome and susceptibility to bisphosphonate-associated osteonecrosis of the jaw. *J. Transl. Med.* 13:212.

Kennedy EA, King KY, Baldridge MT (2018). Mouse Microbiota Models: Comparing Germ-Free Mice and Antibiotics Treatment as Tools for Modifying Gut Bacteria. *Front. Physiol.* 9:1534.

Kim S, Williams DW, Lee C, Kim T, Arai A, Shi S, et al. (2017). IL-36 Induces Bisphosphonate-Related Osteonecrosis of the Jaw-Like Lesions in Mice by Inhibiting TGF-β-Mediated Collagen Expression. *J. Bone Miner. Res.* 32:309–318.

Kim T, Kim S, Song M, Lee C, Yagita H, Williams DW, et al. (2018). Removal of Pre-Existing Periodontal Inflammatory Condition before Tooth Extraction Ameliorates Medication-Related Osteonecrosis of the Jaw-Like Lesion in Mice. *Am. J. Pathol.* 188:2318–2327.

Kos M, Brusco D, Kuebler J, Engelke W (2010). Clinical comparison of patients with osteonecrosis of the jaws, with and without a history of bisphosphonates administration. *Int J Oral Maxillofac Surg* 39:1097–1102.

Marx RE, Cillo JE, Ulloa JJ (2007). Oral bisphosphonate-induced osteonecrosis: risk factors, prediction of risk using serum CTX testing, prevention, and treatment. *J. Oral Maxillofac. Surg.* 65:2397–2410.

Marx RE, Sawatari Y, Fortin M, Broumand V (2005). Bisphosphonate-induced exposed bone (osteonecrosis/osteopetrosis) of the jaws: risk factors, recognition, prevention, and treatment. *J. Oral Maxillofac. Surg.* 63:1567–1575.

Nicolatou-Galitis O, Migkou M, Psyrri A, Bamias A, Pectasides D, Economopoulos T, et al. (2012). Gingival bleeding and jaw bone necrosis in patients with metastatic renal cell carcinoma receiving sunitinib: report of 2 cases with clinical implications. *Oral Surg. Oral Med. Oral Pathol. Oral Radiol.* 113:234–238.

Ohlsson C, Sjögren K (2015). Effects of the gut microbiota on bone mass. *Trends Endocrinol. Metab.* 26:69–74.

Pushalkar S, Li X, Kurago Z, Ramanathapuram LV, Matsumura S, Fleisher KE, et al. (2014). Oral microbiota and host innate immune response in bisphosphonate-related osteonecrosis of the jaw. *Int. J. Oral Sci.* 6:219–226.

Reikvam DH, Erofeev A, Sandvik A, Grcic V, Jahnsen FL, Gaustad P, et al. (2011). Depletion of murine intestinal microbiota: effects on gut mucosa and epithelial gene expression. *PLoS One* 6:e17996.

Ripamonti CI, Maniezzo M, Campa T, Fagnoni E, Brunelli C, Saibene G, et al. (2009). Decreased occurrence of osteonecrosis of the jaw after implementation of dental preventive measures in solid tumour patients with bone metastases treated with bisphosphonates. The experience of the National Cancer Institute of Milan. *Ann. Oncol.* 20:137–145.

Rovin S, Costich ER, Gordon HA (1966). The influence of bacteria and irritation in the initiation of periodontal disease in germfree and conventional rats. *J. Periodontal Res.* 1:193–204.

Ruggiero SL, Dodson TB, Fantasia J, Goodday R, Aghaloo T, Mehrotra B, et al. (2014). American Association of Oral and Maxillofacial Surgeons position paper on medication-related osteonecrosis of the jaw--2014 update. *J. Oral Maxillofac. Surg.* 72:1938–1956.

Sedghizadeh PP, Kumar SKS, Gorur A, Schaudinn C, Shuler CF, Costerton JW (2008). Identification of microbial biofilms in osteonecrosis of the jaws secondary to bisphosphonate therapy. *J. Oral Maxillofac. Surg.* 66:767–775.

Shreiner AB, Kao JY, Young VB (2015). The gut microbiome in health and in disease. *Curr. Opin. Gastroenterol.* 31:69–75.

Sjögren K, Engdahl C, Henning P, Lerner UH, Tremaroli V, Lagerquist MK, et al. (2012). The gut microbiota regulates bone mass in mice. *J. Bone Miner. Res.* 27:1357–1367.

Soave O, Brand CD (1991). Coprophagy in animals: a review. *Cornell Vet* 81:357–364.

Soundia A, Hadaya D, Esfandi N, Gkouveris I, Christensen R, Dry SM, et al. (2018). Zoledronate Impairs Socket Healing after Extraction of Teeth with Experimental Periodontitis. *J. Dent. Res.* 97:312–320.

Tong M, Jacobs JP, McHardy IH, Braun J (2014). Sampling of intestinal microbiota and targeted amplification of bacterial 16S rRNA genes for microbial ecologic analysis. *Curr. Protoc. Immunol.* 107:7.41.1–11.

van 't Hof RJ, Rose L, Bassonga E, Daroszewska A (2017). Open source software for semi-automated histomorphometry of bone resorption and formation parameters. *Bone* 99:69–79.

Williams DW, Lee C, Kim T, Yagita H, Wu H, Park S, et al. (2014). Impaired bone resorption and woven bone formation are associated with development of osteonecrosis of the jaw-like lesions by bisphosphonate and anti-receptor activator of NF-κB ligand antibody in mice. *Am. J. Pathol.* 184:3084–3093.

Yan J, Herzog JW, Tsang K, Brennan CA, Bower MA, Garrett WS, et al. (2016). Gut microbiota induce IGF-1 and promote bone formation and growth. *Proc. Natl. Acad. Sci. USA* 113:E7554–E7563.

Chapter 4

Summary and Conclusions

Oral mucosal wound healing is a complex but critical process following dentoalveolar surgery that protects the host by re-establishing barrier integrity. MRONJ is a condition that results in a non-healing oral wound following dental surgery in some patients taking antiresorptive or antiangiogenic medication. Building upon our previous work on MRONJ pathophysiology and mechanism, here we investigated two confounding factors that lead to the development of MRONJ. The careful manipulation of variables in this work has resulted in a better understanding of the complexity involved in this multifactorial disease process.

In Chapter 2, we assessed the role of chronic periodontal disease in the development of osteonecrosis. We found that the increase in alveolar bone loss between acute and chronic periodontal disease is not a function of the number or type of local microbes, but rather, is associated with high local expression of *Il17a*, and an increase in osteoclasts and $CD3^+$ T cells. When we assessed the role of chronic periodontal disease in MRONJ pathogenesis, we found significant development of necrotic bone that was exacerbated by longer periods of pre-existing periodontal disease. We also identified two potential systemic markers of periodontal disease that may help identify patients at risk of developing MRONJ prior to dental surgery.

In Chapter 3, we studied the function of the commensal microbiota in osteomucosal healing. By depleting the commensal microbiota with high-dose and broad-spectrum antibiotics, we identified that the oral microbiota exerts a catabolic effect on alveolar bone in a ligature model of periodontal disease. Dysbiosis had no effect on MRONJ development following extraction of a healthy tooth, however, local and systemic inhibition of bone resorption by antibiotics and BP, respectfully, led to an increase in bone necrosis following extraction of a diseased tooth.

Our findings have broad implications for future studies on MRONJ pathogenesis. It is abundantly clear from our studies that resolution of dental disease (*e.g.* peri-radicular inflammation) is critical prior to starting antiresorptive treatment. Moreover, we and others have found that necrotic bone begins to form adjacent to diseased teeth prior to extraction,

showcasing the importance of dental health maintenance for any patient with a history of antiresorptive therapy. In addition, our understanding of how the commensal microbiota modifies oral health and homeostasis is in its infancy, and we found that ablation of the microbiota can increase the amount of bone necrosis in a periodontal disease MRONJ model. Our findings suggest that long-term use of broad-spectrum antibiotics may lead to adverse effects in the context of MRONJ development.